The Astrophysical Journal, 747:102 (19pp), 2012 March 10 doi:10.1088/0004-637X/747/2/102

THE GALACTIC R CORONAE BOREALIS STARS: THE C_2 SWAN BANDS, THE CARBON PROBLEM, AND THE $^{12}C/^{13}C$ RATIO

B. P. Hema[1], Gajendra Pandey[1], and David L. Lambert[2]
[1] Indian Institute of Astrophysics, Bangalore Karnataka 560034, India; hema@iiap.res.in, pandey@iiap.res.in
[2] The W.J. McDonald Observatory, University of Texas at Austin, Austin, TX 78712-1083, USA; dll@astro.as.utexas.edu
Received 2011 December 4; accepted 2012 January 4; published 2012 February 21

ABSTRACT

Observed spectra of R Coronae Borealis (RCB) and hydrogen-deficient carbon (HdC) stars are analyzed by synthesizing the C_2 Swan bands (1, 0), (0, 0), and (0, 1) using our detailed line list and the Uppsala model atmospheres. The (0, 1) and (0, 0) C_2 bands are used to derive the ^{12}C abundance, and the (1, 0) $^{12}C^{13}C$ band to determine the $^{12}C/^{13}C$ ratios. The carbon abundance derived from the C_2 Swan bands is about the same for the adopted models constructed with different carbon abundances over the range 8.5 (C/He = 0.1%) to 10.5 (C/He = 10%). Carbon abundances derived from C I lines are about a factor of four lower than the carbon abundance of the adopted model atmosphere over the same C/He interval, as reported by Asplund et al., who dubbed the mismatch between adopted and derived C abundance as the "carbon problem." In principle, the carbon abundances obtained from C_2 Swan bands and that assumed for the model atmosphere can be equated for a particular choice of C/He that varies from star to star. Then, the carbon problem for C_2 bands is eliminated. However, such C/He ratios are in general less than those of the extreme helium stars, the seemingly natural relatives to the RCB and HdC stars. A more likely solution to the C_2 carbon problem may lie in a modification of the model atmosphere's temperature structure. The derived carbon abundances and the $^{12}C/^{13}C$ ratios are discussed in light of the double degenerate and the final flash scenarios.

Key words: stars: abundances – stars: chemically peculiar – stars: evolution

Online-only material: color figures, machine-readable table

1. INTRODUCTION

R Coronae Borealis (RCB) stars are a rare class of F- and G-type supergiants with remarkable photometric and spectroscopic peculiarities. The photometric peculiarity is that an RCB may fade rapidly in visual brightness by up to several magnitudes at unpredictable times and slowly return back to maximum light after an interval of weeks, months, or even years. Most RCB stars stay for a longer time at maximum light than at minimum light. This fading is generally attributed to the formation of dust in the line of sight. Spectroscopic peculiarities are led by the very weak or undetectable hydrogen Balmer lines in their spectra. This indicates that they have a very H-poor atmosphere. This hydrogen deficiency but not the propensity to undergo optical declines is shared by other rare classes of stars: extreme helium (EHe) stars at the hotter end and hydrogen-deficient carbon (HdC) stars at the cooler end of the RCB temperature range.

Keys to understanding origins of RCB stars and their putative relatives have come from the determination and interpretation of the stars' surface chemical compositions. Two proposed scenarios remain in contention. In one dubbed the double degenerate (DD) scenario, a helium white dwarf merges with a carbon–oxygen (C–O) white dwarf (Webbink 1984; Iben & Tutukov 1985). The close white dwarf binary results from mass exchange and mass loss of a binary system as it evolves from a pair of main-sequence stars. The final step to the merger is driven by loss of angular momentum by gravitational waves (Renzini 1979). The envelope of the merged star is inflated to supergiant dimensions for a brief period. An alternative scenario dubbed the final flash (FF) scenario involves a single post-asymptotic giant branch (AGB) star experiencing a final helium shell flash which causes the H-rich envelope to be ingested by the He shell. The result is that the star becomes a hydrogen-deficient supergiant for a brief period and is sometimes referred in this condition as a born-again AGB star (Renzini 1990).

For the RCB stars, determination of chemical compositions by Lambert & Rao (1994) and Asplund et al. (2000) suggested that the DD rather than the FF scenario gave a superior accounting of the determined elemental abundances. This conclusion has since been supported by the determination from analysis of CO infrared bands of a high ^{18}O (relative to ^{16}O) in cool RCBs and HdC stars (Clayton et al. 2005, 2007; García-Hernández et al. 2009, 2010). Additional evidence comes from high fluorine abundances in EHe (Pandey 2006) and RCB stars (Pandey et al. 2008).

In the case of the RCB stars, there is an unease about the results for the elemental abundance on account of "the carbon problem" identified and discussed by Asplund et al. (2000). Since the continuous opacity in the optical is predicted to arise from the photoionization of neutral carbon from highly excited states, the strength of an optical C I line, also from a highly excited state, is predicted to be quasi-independent of atmospheric parameters such as effective temperature, surface gravity, and metal abundance. Indeed, a C I line has a nearly constant strength across the RCB sample even as, for example, an Fe I or an Fe II line may vary widely in strength from one star to the next. However, the predicted strength of a C I line is much stronger than its observed strength: if one were to choose to resolve this discrepancy by adjusting the line's gf-value, it must be reduced by a factor of four or 0.6 dex on average. This discrepancy between predicted and observed C I line strengths is termed "the carbon problem." Adjustment of the gf-values of the C I lines is not the only potential or even the preferred way to address the carbon problem.

In this paper, we present and discuss spectra showing the C_2 Swan bands in a sample of RCB and HdC stars. Our first

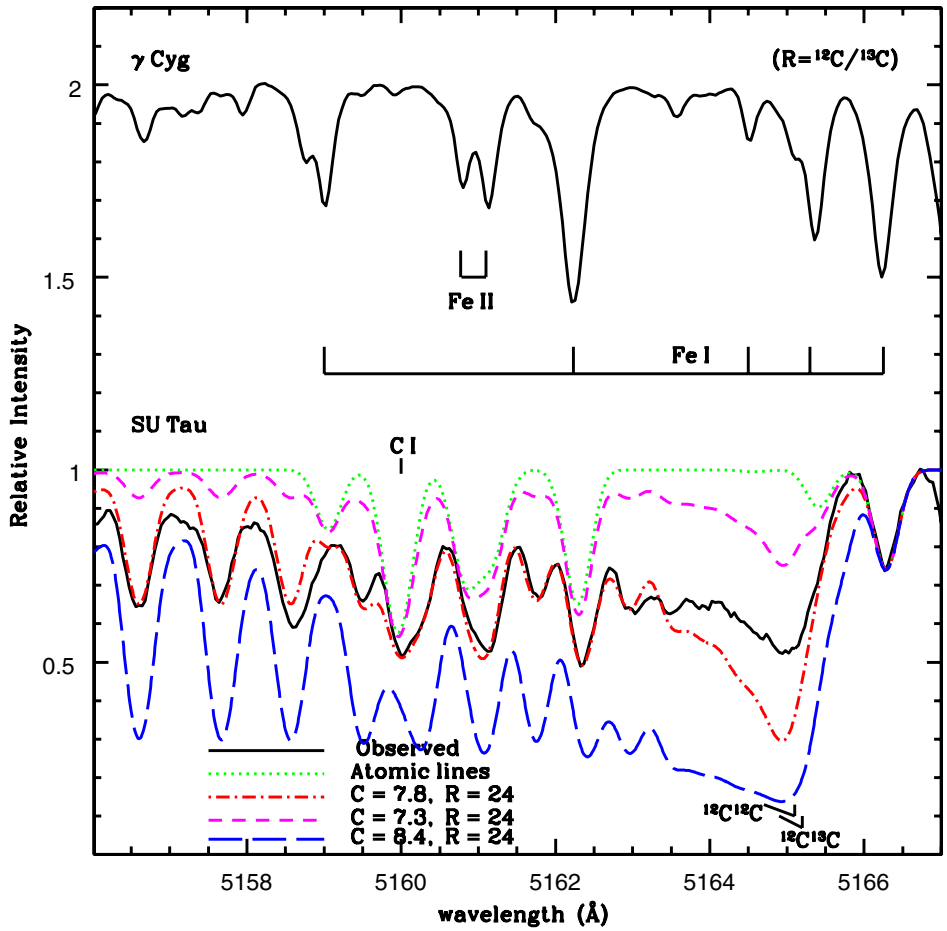

Figure 1. Observed and synthetic spectra of the (0, 0) C_2 band for SU Tau. Synthetic spectra are plotted for different values of the C abundance—see key on the figure. The spectrum of the γ Cyg is plotted with the positions of the key lines marked.
(A color version of this figure is available in the online journal.)

goal is to compare predicted and observed strengths of C_2 Swan bands in RCB stars to see if they exhibit a carbon problem and if that problem differs from that shown by the C I lines. Our second goal is to look for $^{12}C^{13}C$ lines and determine the $^{12}C/^{13}C$ ratio. A high value of $^{12}C/^{13}C$ ratio is expected for the DD scenario, but a low ratio seems likely for the FF scenario. High ratios or high lower limits on the isotopic ratio have been set for HdC stars: HD 137613 (Fujita & Tsuji 1977) and HD 182040 (Climenhaga 1960; Fujita & Tsuji 1977). A limit of greater than 40 was set for R CrB (Cottrell & Lambert 1982). But the RCB star V CrA is apparently an exception with a reported low value of $^{12}C/^{13}C$ ratio: Rao & Lambert (2008) estimated the ratio at 4–10 for V CrA.

As expected, a low value of $^{12}C/^{13}C$ ratio is shown by the FF object V4334 Sgr (Sakurai's object), the ratio is 2–5 (Asplund et al. 1997b; Pavlenko et al. 2004). However, the other objects which are thought to be FF objects, such as FG Sge (Gonzalez et al. 1998) and V605 Aql (Lundmark 1921; Clayton & De Marco 1997), do not show the presence of $^{12}C^{13}C$ bands in their spectrum.

2. OBSERVATIONS

High-resolution optical spectra of RCB/HdC stars at maximum light were obtained from the W. J. McDonald Observatory and the Vainu Bappu Observatory. The dates of observations, the visual validated magnitudes (AAVSO[3]), and the signal-to-noise ratio (S/N) per pixel of the spectra in the continuum near

Table 1
Log of the Observations

Star	Date of Observation	V	Observatory	S/N
V3795 Sgr	1996 Jul 26	11.2	McDonald	110
XX Cam	2002 Nov 17	7.4	McDonald	200
VZ Sgr	2007 May 22	10.2	McDonald	200
UX Ant	2007 May 5	12.8	McDonald	120
RS Tel	2010 May 28/29	9.9	VBT	25
R CrB	2007 May 5	6.0	McDonald	200
V2552 Oph	2007 May 22	11.0	McDonald	128
V854 Cen	2010 May 24–27/1999 Feb 10	7.25	VBT/McDonald	250
V482 Cyg	2007 May 23/24	10.8	McDonald	152
SU Tau	2002 Nov 15	9.8	McDonald	196
V CrA	2003 Sep 6	9.5	McDonald	137
GU Sgr	2007 May 23	11.1	McDonald	135
FH Sct	2007 May 24	12.1	McDonald	87
U Aqr	1996 Jul 23	11.2	McDonald	125
HD 173409	2010 May 27	9.5	VBT	70
HD 182040	2010 May 25	7.0	VBT	110
HD 175893	2010 May 25	9.3	VBT	30
HD 137613	2010 May 24	7.5	VBT	90

Note. The stars are listed in the decreasing order of their effective temperature from top to bottom.

[3] http://www.aavso.org

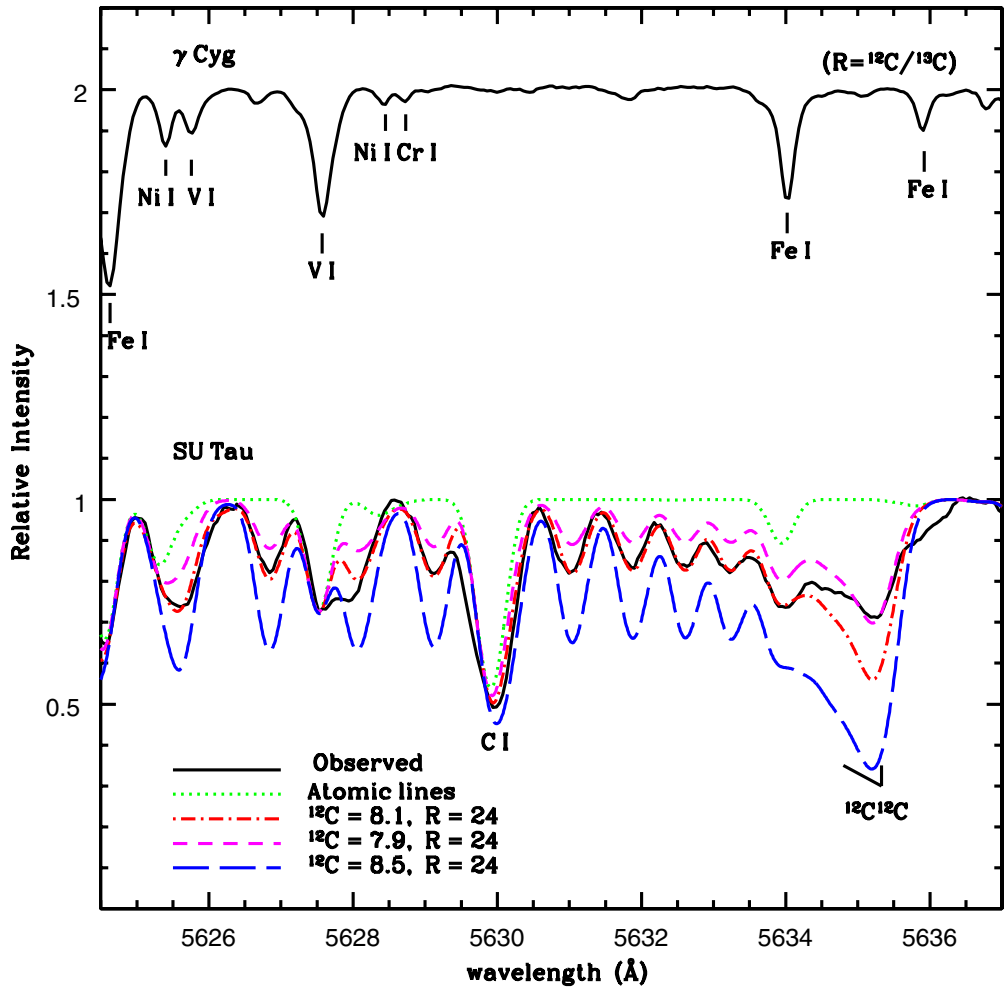

Figure 2. Observed and synthetic spectra of the (0, 1) C_2 band for SU Tau. Synthetic spectra are plotted for different values of the C abundance—see key on the figure. The spectrum of the γ Cyg is plotted with the positions of the key lines marked.
(A color version of this figure is available in the online journal.)

Table 2
Sample Lines for (1, 0) C_2 Swan Band

Wavelength (Å)	J''	χ (eV)	log gf
4692.348	28.0	0.342	−0.270
4692.485	28.0	0.342	−0.270
4692.548	27.0	0.342	−0.286
4692.679	26.0	0.342	−0.302
4692.794	61.0	0.940	0.064
4692.838	61.0	0.940	0.064
4692.848	62.0	0.940	0.071
4692.931	60.0	0.940	0.057
4693.077	60.0	0.940	0.057
4694.391	27.0	0.331	−0.286

(This table is available in its entirety in a machine-readable form in the online journal. A portion is shown here for guidance regarding its form and content.)

the 4737 Å $^{12}C_2$ bandhead are given in Table 1. In addition to the RCB stars, a spectrum of γ Cyg was obtained at the McDonald Observatory. This F5Ib star is of similar spectral type to the warm RCBs such as R CrB.

The spectra from the McDonald Observatory were obtained with the 2.7 m Harlan J. Smith Telescope and Tull coudé cross-dispersed echelle spectrograph (Tull et al. 1995) at a resolving power of $\lambda/d\lambda = 60{,}000$. The spectra from the Vainu Bappu Observatory were obtained with the 2.34 m Vainu Bappu Telescope (VBT) equipped with the fiber-fed cross-dispersed echelle spectrometer (Rao et al. 2005) and a 4 × 4 K CCD are at a resolving power of about 30,000.

3. SPECTRUM SYNTHESIS

Our analysis of the high-resolution spectra proceeds by fitting synthetic spectra to the observed spectra in several bandpasses providing lines of the C_2 Swan system. For the synthesis of the C_2 Swan bands, we use model atmospheres and as complete a line list as possible. In the following subsections, we introduce the line lists for the C_2 Swan bands and the atomic lines blended with the C_2 bands and, finally, the procedure for computing the synthetic spectra.

3.1. The Swan Bands

The C_2 Swan bands are detectable in all but the hottest RCB stars. They are not seen in either V3795 Sgr or XX Cam with effective temperatures of 8000 K and 7250 K, respectively. In our sample, they are first detectable in VZ Sgr at $T_{\rm eff} = 7000$ K. The bands are very strong in the coolest RCB stars like U Aqr and the HdC stars. The leading bands of the three sequences

Table 3
The Atomic Line List Used in the Syntheses of the (1, 0) C_2 Swan Band Region with the Individual Estimates of the Log gf-values from the γ Cyg, Sun, and Arcturus Spectra and the Adopted Log gf-values

Line	χ (eV)	log $gf_{\gamma\ \mathrm{Cyg}}$[a]	log gf_{Sun}[b]	log gf_{Arcturus}[c]	log gf_{Source}	Source	log gf_{adopted}
Fe I λ4729.018	4.07	−1.72	−1.60	−1.70	−1.61	NIST	−1.72
Ni I λ4729.280	4.10	−2.00	−1.20	...	−1.20	NIST	−2.00
Fe I λ4729.676	3.40	−2.36	−2.32	−2.50	−2.42	NIST	−2.36
Mg I λ4730.028	4.34	−2.49	−2.42	−2.49	−2.34	NIST	−2.49
Cr I λ4730.710	3.08	−0.48	−0.38	−0.38	−0.19	NIST	−0.48
Ti I λ4731.165	2.17	...	−0.51	−0.51	−0.41	Kurucz	−0.51
Ni I λ4731.798	3.83	...	−0.93	−1.10	−0.85	NIST	−0.93
Ni I λ4732.457	4.10	−0.59	−0.55	...	−0.55	NIST	−0.59
Ti I λ4733.421	2.16	...	−0.70	−0.65	−0.40	Kurucz	−0.70
Fe I λ4733.591	1.48	−3.17	−3.03	−3.03	−2.98	NIST	−3.17
Fe I λ4734.098	4.29	−1.60	−1.57	−1.43	−1.56	NIST	−1.60
C I λ4734.260	7.94	...	...	...	−2.36	NIST	...
Ti I λ4734.670	2.24	...	−0.87	−0.87	−0.86	Kurucz	−0.87
C I λ4734.917	7.94	...	...	...	−4.29	NIST	...
C I λ4735.163	7.94	...	...	...	−3.11	NIST	...
Fe I λ4735.843	4.07	−1.12	−1.22	−1.32	−1.22	Kurucz	−1.12
Fe I λ4736.773	3.21	−0.88	−0.75	−0.90	−0.75	NIST	−0.88
Cr I λ4737.355	3.09	0.00	−0.30	−0.30	−0.09	NIST	0.00
Fe I λ4737.635	3.26	−2.55	−2.50	−2.45	−2.24	Kurucz	−2.55
C I λ4738.213	7.94	...	...	...	−3.11	NIST	...
C I λ4738.460	7.94	...	...	...	−2.63	NIST	...
Mn I λ4739.110	2.94	−0.48	−0.62	−0.70	−0.49	NIST	−0.48
Zr I λ4739.480	0.65	−0.13	−0.13	−0.13	0.23	Kurucz	−0.13
Mg II λ4739.588	11.56	−0.20	...	...	−0.66	NIST	−0.20
Ni I λ4740.165	3.48	−1.33	−1.83	−1.85	−1.90	NIST	−1.33
Fe I λ4740.340	3.01	−1.90	−2.67	−2.75	−2.63	NIST	−1.90
Sc I λ4741.024	1.43	0.98	0.94	0.84	2.27	NIST	0.98
Fe I λ4741.067	3.33	−2.48	−2.45	−2.50	−2.76	Kurucz	−2.48
Fe I λ4741.530	2.83	−2.10	−2.10	−2.50	−1.76	NIST	−2.10
Ti I λ4742.106	2.15	−3.96	−3.96	−3.92	−0.67	Kurucz	−3.96
C I λ4742.561	7.94	...	...	...	−2.99	NIST	...
Ti I λ4742.800	2.24	−0.09	0.01	−0.09	0.21	NIST	−0.09
Fe I λ4742.932	4.19	−2.16	−2.36	−2.23	−2.36	Kurucz	−2.16
Fe I λ4744.387	4.50	−0.90	−1.00	−1.10	−1.18	ccp7	−0.90
Fe I λ4744.942	3.26	−2.45	−2.42	−2.40	−2.38	Kurucz	−2.45
Fe I λ4745.128	2.22	−4.10	−4.05	−4.10	−4.08	NIST	−4.10
Fe I λ4745.799	3.65	−1.25	−1.30	−1.40	−1.27	NIST	−1.25
Fe I λ4749.947	4.55	−1.33	−1.33	−1.33	−1.33	NIST	−1.33
Fe I λ4765.480	1.60	−3.81	−3.81	−3.70	−4.01	Kurucz	−3.81
Fe I λ4786.806	3.01	−1.60	−1.60	−1.65	−1.60	NIST	−1.60
Fe I λ4787.826	2.99	−2.56	−2.56	−2.50	−2.60	NIST	−2.56
Fe I λ4788.756	3.23	−1.76	−1.76	−1.76	−1.76	NIST	−1.76
Fe I λ4789.650	3.54	−1.16	−1.16	−1.20	−0.96	NIST	−1.16
Fe I λ4799.405	3.63	−1.89	−1.89	−1.93	−2.19	NIST	−1.89
Fe I λ4802.879	3.64	−1.51	−1.51	−1.51	−1.51	NIST	−1.51
Fe I λ4808.148	3.25	−2.84	−2.84	−2.70	−2.74	NIST	−2.84
Fe I λ4809.938	3.57	−2.08	−2.10	−2.15	−2.60	NIST	−2.08

Notes.
[a] MARCS Model atmosphere with atmospheric parameters and abundances from Luck & Lambert (1981).
[b] MARCS Model atmosphere with atmospheric parameters and abundances from Asplund et al. (2009).
[c] MARCS Model atmosphere with atmospheric parameters and abundances from Peterson et al. (1993).

$\Delta v = +1$, 0, and −1 are each considered. All bands have blue-degraded bandheads. The (0, 0) band of the $^{12}C_2$ molecule with its head at 5165 Å is the strongest band of the entire Swan system. The (1, 0) and (0, 1) bandheads are at 4737 Å and 5636 Å, respectively. All three bands are synthesized using detailed line lists including the blending atomic lines and appropriate model atmospheres. The (1, 0), (0, 0), and (0, 1) $^{12}C_2$ bands are used to determine the C abundance and, hence, to assess the carbon problem. The (0, 1) band is generally a superior indicator of the C abundance because it is less affected by blending atomic lines. However, the (1, 0) band is the focus of efforts to determine the $^{12}C/^{13}C$ ratio because the $^{12}C^{13}C$ bandhead is shifted to 4745 Å and, thus, 8 Å clear of the blue-degraded $^{12}C_2$ band. For the (0, 0) and (0, 1) bands, the $^{12}C^{13}C$ lines are mixed among the stronger $^{12}C_2$ lines.

Data required for synthesis of Swan bands include wavelengths of the transitions, excitation energies of the lower levels, gf-values of the lines, and the C_2 molecule's dissociation energy. Accurate wavelengths for $^{12}C_2$ lines are taken from Phillips & Davis (1968). Excitation energies are computed from

the molecular constants given by the latter reference. The wavelength shift between a $^{12}C^{13}C$ line and the corresponding $^{12}C_2$ line is calculated using standard formulae for the vibrational and rotational shifts (Herzberg & Phillips 1948; Stawikowski & Greenstein 1964; Russo et al. 2011). Predictions for the bandhead wavelength shifts were checked against the measurements by Pesic et al. (1983).

gf-values are calculated from the theoretical band oscillator strengths computed by Schmidt & Bacskay (2007): $f(1, 0) = 0.009414$, $f(0, 0) = 0.03069$, and $f(0, 1) = 0.01015$. These theoretical computations predict radiative lifetimes for the upper state of the Swan system that are within a few percent of the accurate measurements by laser-induced fluoresence reported by Naulin et al. (1988). The C_2 dissociation energy is taken from an experiment involving multi-photon dissociation of acetylene: $D_0(C_2) = 6.297$ eV (Urdahl et al. 1991). Our molecular data for individual $^{12}C_2$ lines—gf-values and excitation energies—are in excellent agreement with values listed by Asplund et al. (2005) for their determination of the solar C abundance. Detailed molecular line lists used in our analyses of C_2 bands, including the wavelengths, J-values of the lower level, the lower excitation potentials, and the log gf-values, are published in the online journal (see sample Table 2, which gives some lines of (1, 0) $^{12}C_2$ band).

3.2. Atomic Lines

In order to ensure a satisfactory synthesis of an RCB spectrum, an accounting for the atomic lines at the wavelengths covered by the C_2 bands is necessary, most especially for the (1, 0) $^{12}C^{13}C$ bandhead which is always weak and generally seriously blended. The region 4729–4748 Å was given special attention. The procedure applied to the (1, 0) band was followed for the (0, 0) and (0, 1) bands.

Prospective atomic lines were first compiled from the usual primary sources: the Kurucz database,[4] the NIST database,[5] the VALD database[6], and the comprehensive multiplet table for Fe I (Nave et al. 1994). Our next step was to identify the atomic lines in the spectrum of γ Cyg, Arcturus, and the Sun and to invert their equivalent widths to obtain the product of a line's gf-value and the element's abundance. For lines of a given species (e.g., Fe I), the assumption is that the relative gf-values obtained from these sources may be applied to an RCB spectrum synthesis but an adjustment may be needed to allow for an abundance difference between the source and the RCB. After the adjustment for abundance differences between the sources, the gf-values are in agreement within 0.1 dex (see Table 3 for the individual estimates of the gf-values as well as the adopted value). For most lines the gf-values adopted are those derived from γ Cyg spectrum. For the lines which are not resolved in γ Cyg spectrum, the gf-values are adopted from the solar spectrum.

Lines of C I present in all RCB spectra are not present in the reference spectra of γ Cyg, Arcturus, and the Sun. The C I lines were identified using Moore's (1993) multiplet table with gf-values taken from the NIST database. A C I line is betrayed by the fact that a given C I line has a similar strength in all RCB spectra. In this regard, the feature coincident with the $^{12}C^{13}C$ (1, 0) bandhead is unlikely to be a very weak unidentified C I line because its strength varies from star to star. Note, for example, the absence or near-absence of this line in the spectra of V3795 Sgr and V854 Cen. Furthermore, this line is stronger in the spectrum of γ Cyg, where the C I lines are very weak.

[4] http://kurucz.harvard.edu
[5] http://www.nist.gov
[6] http://vald.astro.univie.ac.at

Table 4
The Fe Abundances for RCB and HdC Stars

Star	logϵ(Fe)[a]	logϵ(Fe)[b]	logϵ(Fe)[c]
V3795 Sgr	5.7(0.3)(3)	5.6	<6.0
XX Cam	6.8(0.3)(5)	6.8	6.8
VZ Sgr	6.1(0.3)(4)	5.8	7.2
UX Ant	6.2(0.15)(5)	6.2	7.0
RS Tel	6.5(0.2)(3)	6.4	6.9
R CrB	6.6(0.2)(5)	6.5	7.0
V2552 Oph	6.6(0.2)(4)	6.4	6.9
V854 Cen	5.0(0.3)(3)	5.0	6.5
V482 Cyg	6.7(0.15)(5)	6.7	6.9
SU Tau	6.1(0.3)(4)	6.1	6.5
V CrA	5.5(0.1)(3)	5.5	6.6
GU Sgr	6.5(0.25)(6)	6.3	6.8
FH Sct	6.4(0.15)(5)	6.3	6.8
U Aqr	6.5(0.30)(8)	...	7.3
HD 173409	6.6(0.3)(10)	6.8	6.6
HD 182040	6.6(0.25)(9)	6.9	6.4
HD 175893	6.7(0.2)(5)	6.8	6.7
HD 137613	6.8(0.20)(9)	6.6	6.7

Notes.
[a] From the 4700 Å region, the values in parentheses are the standard deviation and the number of lines used, respectively.
[b] From Asplund et al. (2000) for RCB stars and from Warner (1967) for HdC stars.
[c] From the 4744.4 Å line, assuming it to be entirely Fe I.

Initially, elemental abundances for RCB stars were adopted from Asplund et al. (2000) and Rao & Lambert (2003). Then, equivalent widths were measured off our spectra and the abundances redetermined for RCB stars were found to be in good agreement with Asplund et al. (2000). In particular, we derived the Fe abundance from lines in the 4745–4810 Å window where C_2 contamination is minimal. The Fe abundances derived from these Fe I lines are in good agreement with the Fe abundances derived by Asplund et al. (2000; see Table 4). These Fe abundances were adopted for deriving the $^{12}C/^{13}C$ ratios in RCB stars. The uncertainties on the Fe abundance are used to derive the upper and lower limits to $^{12}C/^{13}C$ ratios in RCB stars (including U Aqr). The metal abundances for the synthetic spectra are adopted from Asplund et al. (2000) for most of the stars. However, for V2552 Oph we adopt the abundances from Rao & Lambert (2003). We also assume the solar relative abundances with the correction of about +0.3 dex for the α-elements at these metallicities, if these abundances are not measured in these stars. Fe abundances are derived also for HdC stars and the cool RCB U Aqr.

3.3. Spectrum Synthesis of the C_2 Bands

For the spectrum synthesis, we used the line-blanketed H-deficient model atmospheres by Asplund et al. (1997a) and the UPPSALA spectrum synthesis BSYNRUN program. For equivalent width analysis we used EQWRUN program. The appropriate model atmosphere for a given RCB star was chosen using the stellar parameters from Asplund et al. (2000): effective temperature $T_{\rm eff}$, surface gravity log g, and microturbulence ξ_t.

The stellar parameters for the cool RCB star U Aqr and HdC stars are adopted from Asplund et al. (1997a) and García-Hernández et al. (2009, 2010) and used with the MARCS model

Table 5
The Derived Carbon Abundances for RCB Stars from (0, 0), (0, 1) and (1, 0) C_2 Bands

Stars	logϵ(C) from (0, 1) C_2 band			logϵ(C) from (0, 0)			logϵ(C) from (1, 0)			logϵ(C) from C I lines
	C/He = 0.3% log ϵ(C) = 9.0	C/He = 1.0% log ϵ(C) = 9.5	C/He = 3.0% log ϵ(C) = 10.0	C/He = 0.3% log ϵ(C) = 9.0	C/He = 1.0% log ϵ(C) = 9.5	C/He = 3.0% log ϵ(C) = 10.0	C/He = 0.3% log ϵ(C) = 9.0	C/He = 1.0% log ϵ(C) = 9.5	C/He = 3.0% log ϵ(C) = 10.0	C/He = 1.0% log ϵ(C) = 9.5
VZ Sgr	9.0	8.9	8.8	9.0	8.8	8.7	9.0	8.8	8.6	8.9
UX Ant	8.4	8.3	8.2	8.2	8.1	8.0	8.4	8.1	8.0	8.7
RS Tel	...	...	...	8.4	8.3	8.3	8.7	8.5	8.4	8.7
R CrB	9.0	8.8	8.8	8.9	8.6	8.6	9.0	8.8	8.7	8.9
V2552 Oph	8.3	8.1	8.2	8.1	8.1	8.1	8.1	8.0	7.9	8.7
V854 Cen	8.4	8.3	8.3	8.4	8.3	8.2	...	8.5	8.2	8.8
V482 Cyg	8.4	8.3	8.3	8.2	8.1	8.1	8.2	8.2	8.1	8.9
SU Tau	8.1	8.0	8.0	7.8	7.8	7.8	7.8	7.7	7.7	8.6
V CrA	8.5	8.4	8.3	8.3	8.2	8.2	8.5	8.4	8.3	8.6
GU Sgr	8.2	8.1	8.1	8.1	8.1	8.1	8.2	8.1	8.0	8.9
FH Sct	7.8	7.7	7.7	7.8	7.8	7.7	7.7	7.7	7.6	8.9

Table 6
The Derived Carbon Abundances for HdC Stars and RCB Star U Aqr from (0, 1) and (1, 0) C_2 Bands

Stars	logϵ(C) from (0, 1) C_2 band			logϵ(C) from (1, 0)			logϵ(C) from C I lines
	C/He = 0.1% log ϵ(C) = 8.5	C/He = 1.0% log ϵ(C) = 9.5	C/He = 10% log ϵ(C) = 10.5	C/He = 0.1% log ϵ(C) = 8.5	C/He = 1.0% log ϵ(C) = 9.5	C/He = 10% log ϵ(C) = 10.5	C/He = 1.0% log ϵ(C) = 9.5
HD 173409	...	8.7	...	...	8.7	...	8.6
HD 182040	8.8	9.0	8.9	8.8	9.0	8.9	9.0
HD 175893	8.9	9.0	8.9	8.8	8.9	8.8	8.5
HD 137613	8.8	9.0	8.9	8.8	9.0	8.9	8.5
U Aqr[a]	...	9.2	...	...	9.2	...	8.9

Note. [a] Adopted ($T_{\rm eff}$, log g) = (5400, 0.5). If ($T_{\rm eff}$, log g) = (6000, 0.5) is adopted, the derived carbon abundance is about 10.4.

atmospheres (Gustafsson et al. 2008) provided by K. Eriksson (2011, private communication) used by García-Hernández et al. (2009, 2010). For the four HdC stars and the cool RCB star U Aqr, we have derived the microturbulence ($\xi_{\rm t}$) from Fe I lines in the region of 4750–4960 Å since there are no significant molecular bands in this wavelength region (Warner 1967). The microturbulent velocity derived from Fe I lines for U Aqr is $\xi_{\rm t} = 5.0 \pm 2$ km s^{-1} and the Fe abundance is log ϵ(Fe) = 6.7 ± 0.3, but adoption of a lower effective temperature, $T_{\rm eff} = 5400$ K, suggested by García-Hernández et al. (2010) gives an Fe abundance of 6.5 ± 0.3. For HdC stars, the derived microturbulent velocities and Fe abundances are: for HD 137613, $\xi_{\rm t} = 6.5 \pm 2$ km s^{-1} and log ϵ(Fe) = 6.8 ± 0.3; for HD 182040, $\xi_{\rm t} = 6.5 \pm 2$ km s^{-1} and log ϵ(Fe) = 6.6 ± 0.3; for HD 173409, $\xi_{\rm t} = 6.0 \pm 2$ km s^{-1} and log ϵ(Fe) = 6.6 ± 0.3; and for HD 175893, $\xi_{\rm t} = 6.0 \pm 2$ km s^{-1} and log ϵ(Fe) = 6.7 ± 0.3. The other stellar parameters, such as $T_{\rm eff}$ and log g, and the elemental abundances are judged from Warner (1967), Asplund et al. (1997a), and García-Hernández et al. (2009).

Stars with effective temperature less than or about 7000 K were selected for the analysis of their C_2 bands. The C_2 molecular bands were synthesized with the line lists discussed above. The synthesized spectrum was convolved with a Gaussian profile with a width that represents the combined effect of stellar macroturbulence and the instrumental profile. The synthesized spectrum is then matched to the observed spectrum by adjustment of the appropriate abundances.

4. THE CARBON ABUNDANCE

If there were no carbon problem for C_2 bands, the ^{12}C abundance derived by fitting each $^{12}C_2$ band would equal the input C abundance of the adopted model atmosphere to within the margin implied by the uncertainties arising from the errors assigned to the model atmosphere parameters. (The changes in spectrum syntheses arising from uncertainties in the basic data for the Swan bands and in the carbon isotopic ratio are negligible.)

In Table 5, the derived C abundances from C_2 bands for the RCB stars are summarized for the three bands and for models with C/He = 0.3%, 1.0%, and 3.0%. Table 6 similarly gives C abundances for the four HdC stars and the cool RCB star U Aqr. In both Tables 5 and 6, we also give the C abundance from the C I lines but only for C/He = 1% models. For a given model, the three bands give the same C abundance to within 0.2 dex, a quantity comparable to the fitting uncertainty. Along the sequence of models from C/He = 0.3% to 3.0%, the derived C abundance decreases by about 0.2 dex for the warmest stars to 0.1 dex for the coolest stars or equivalently the carbon problem increases from the warmest stars to the coolest stars. A carbon problem exists for all models with C/He in the range from 0.3% to 3.0%. Extrapolation of the C abundances in Table 5 to lower input C/He ratio suggests that elimination of the C problem requires models with values of C/He across the range 0.3% (VZ Sgr, R CrB) to 0.03% (V2552 Oph, SU Tau). Table 6 suggests that C/He $\simeq$ 0.3% may account for the HdC stars and cool RCB U Aqr. Adoption of $T_{\rm eff} = 6000$ K for U Aqr suggests C/He of 10%, and not in line with that of HdC stars. Hence, $T_{\rm eff} = 5400$ K is adopted for U Aqr over $T_{\rm eff} = 6000$ K. Discussion of this C/He range is postponed to Section 5.

By way of illustrating the fits of the synthetic spectra to observed spectra for the warm RCB stars, we show synthetic and observed spectra for SU Tau in Figures 1 and 2 for the (0, 0) and (0, 1) C_2 bands, respectively. A corresponding figure for the (1, 0) figure is shown later. The (0, 1), (0, 0), and (1, 0) bands each highlight a different issue. For the HdC stars and the cool RCB U Aqr, the C_2 bands are very strong and the issues are somewhat different and related to the saturation of the lines.

For the (0, 1) band, a ^{12}C abundance is found to fit well the entire illustrated region except that right at the bandhead the observed spectrum is shallower than that predicted. This mismatch is not peculiar to SU Tau and is insensitive to the choice of the C/He ratio. This best fit for SU Tau demands a C abundance of 8.1 or, equivalently, presents a C problem of 0.9 dex; the synthesis with a C abundance of 9.0 (i.e., zero C problem) is obviously a very poor representation of the observed spectrum.

Synthetic spectra for the (0, 0) bands give results essentially identical to those for the (0, 1) bands. The C abundance from the best-fitting synthesis as judged by the fit to the C_2 lines away from the bandhead is within 0.2 dex of the values from the (0, 1) bands. The mismatch between synthesis and observation at the bandhead is greater than for the (0, 1) band and extends over a greater wavelength interval than for the (0, 1) band.

A special difficulty occurs at the (1, 0) $^{12}C_2$ bandhead because there are strong atomic lines at and shortward of the bandhead. A line right at the head is an Fe I line and those shortward of the head are C I lines. These and weaker atomic lines make it difficult to distinguish the C_2 contribution to the spectrum from that of the atomic lines when the C_2 contribution is weak.

As long as the continuous opacity is provided by photoionization of neutral carbon, the carbon problem (see Tables 5 and 6) raised by the C I lines cannot be erased by changes to the stellar parameters. The original carbon problem referred to the mismatch between the observed and predicted strengths of C I lines: the latter were stronger than the former by an amount equivalent to about a 0.6 dex reduction in a line's gf-value. The star-to-star variation in this reduction across the RCB

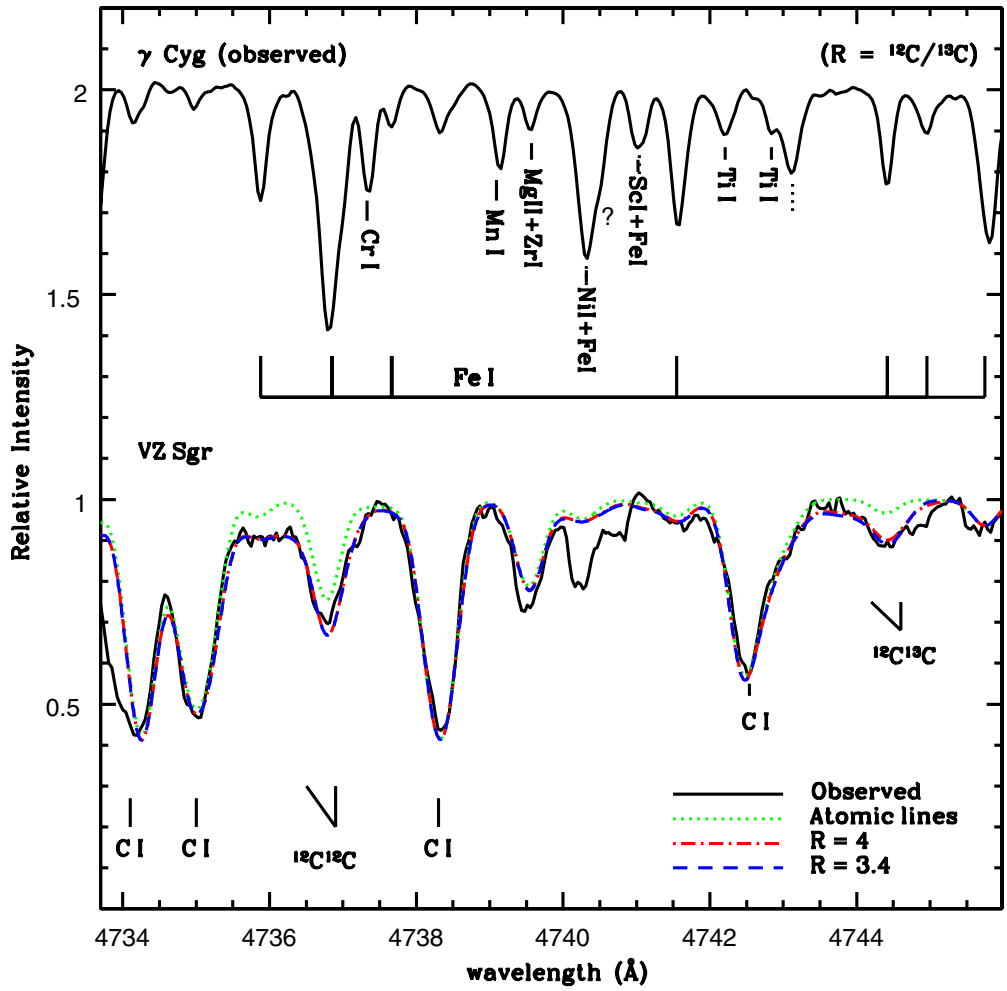

Figure 3. Observed and synthetic spectra of the (1, 0) C_2 bands for VZ Sgr. Synthetic spectra are plotted for the values of the isotopic ratios (R) shown in the keys and for a spectrum with just the atomic lines. The spectrum of γ Cyg is also plotted—the positions of the key lines are also marked—the dotted line represents the blending of one or more atomic lines.

(A color version of this figure is available in the online journal.)

Table 7
The Adopted Stellar Parameters and the $^{12}C/^{13}C$ Ratios for the Analyzed Stars

Star	($T_{\rm eff}$[K], log g[cgs], ξ_t[km s^{-1}])	$^{12}C/^{13}C$ Ratio[a]	$^{12}C/^{13}C$ Ratio
VZ Sgr	(7000, 0.5, 7.0)	3– 6	...
UX Ant	(6750, 0.5, 5.0)	14–20	...
RS Tel	(6750, 1.0, 8.0)	>60	...
R CrB	(6750, 0.5, 7.0)	>40	>40[b]
V2552 Oph	(6750, 0.5, 7.0)	>8	...
V854 Cen	(6750, 0.0, 6.0)	16–24	...
V482 Cyg	(6500, 0.5, 4.0)	>100	...
SU Tau	(6500, 0.5, 7.0)	>24	...
V CrA	(6500, 0.5, 7.0)	8–10	4–10[c]
GU Sgr	(6250, 0.5, 7.0)	>40	...
FH Sct	(6250, 0.0, 6.0)	>14	...
U Aqr	(5400, 0.5, 5.0)	110–120	...
HD 173409	(6100, 0.5, 6.0)	>60	...
HD 182040	(5400, 0.5, 6.5)	>400	>100[d,e]
HD 175893	(5400, 0.5, 6.0)	>100	...
HD 137613	(5400, 0.5, 6.5)	>100	>500[e]

Notes.
[a] Present work.
[b] Cottrell & Lambert (1982).
[c] Rao & Lambert (2008).
[d] Climenhaga (1960).
[e] Fujita & Tsuji (1977).

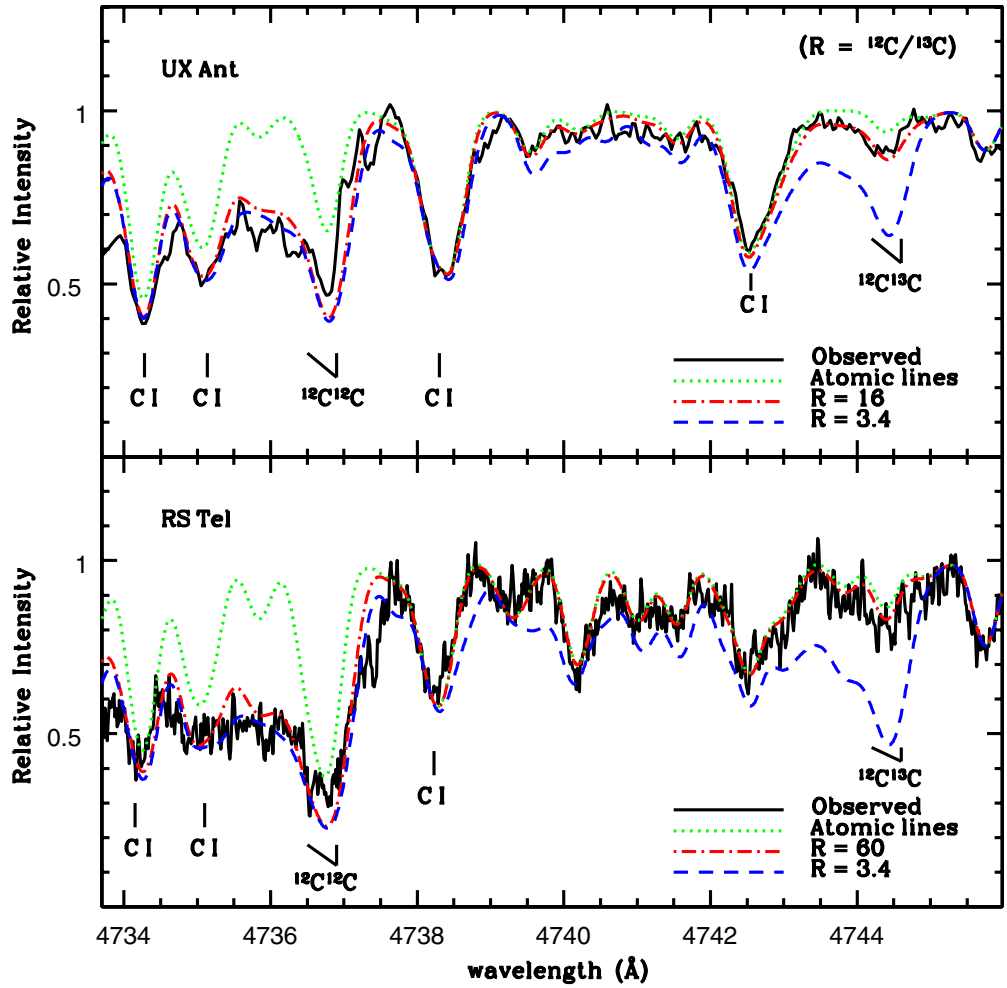

Figure 4. Observed and synthetic spectra of the (1, 0) C_2 bands for UX Ant and RS Tel. Synthetic spectra are plotted for the values of the isotopic ratios (R) shown in the keys and for a spectrum with only the atomic lines. The positions of the key lines are also marked.

(A color version of this figure is available in the online journal.)

Table 8

The Log ϵ(C) from (0,0) and (0, 1) C_2 Bands, Except for RS Tel which Is Only from the (0, 0) C_2 Band, with a C/He Ratio of 1%

Star	($T_{\rm eff}$, log g)	($T_{\rm eff}$-250, log g)	($T_{\rm eff}$, log g)	($T_{\rm eff}$+250, log g)	($T_{\rm eff}$, log g-0.5)	($T_{\rm eff}$, log g)	($T_{\rm eff}$, log g+0.5)	log ϵ (C I)
VZ Sgr	(7000, 0.5)	8.3	8.8	...	...	8.8	8.4	8.9
UX Ant	(6750, 0.5)	7.9	8.3	...	...	8.3	8.0	8.7
RS Tel	(6750, 1.0)	8.1	8.3	...	8.6	8.3	8.2	8.7
R CrB	(6750, 0.5)	8.3	8.8	...	...	8.8	8.4	8.9
V2552 Oph	(6750, 0.5)	7.9	8.1	...	8.5	8.1	8.0	8.7
V854 Cen	(6750, 0.0)	7.8	8.3	...	...	8.3	7.9	8.8
V482 Cyg	(6500, 0.5)	8.1	8.3	8.7	8.6	8.3	8.2	8.9
SU Tau	(6500, 0.5)	7.8	8.0	8.4	8.3	8.0	7.9	8.6
V CrA	(6500, 0.5)	8.2	8.4	8.8	8.7	8.4	8.3	8.6
GU Sgr	(6250, 0.5)	7.9	8.1	8.4	8.3	8.1	8.1	8.9
FH Sct	(6250, 0.0)	7.5	7.7	8.0	7.9	7.7	7.6	8.9
U Aqr	(5400, 0.5)	8.9	9.2	9.5	...	9.2	...	8.9
HD 173409	(6100, 0.5)	8.4	8.7	9.0	...	8.7	...	8.6
HD 182040	(5400, 0.5)	8.7	9.0	9.3	...	9.0	...	9.0
HD 175893	(5400, 0.5)	8.7	9.0	9.3	...	9.0	...	8.5
HD 137613	(5400, 0.5)	8.7	9.0	9.3	...	9.0	...	8.5

sample was small: for example, the C I problem for the 10 stars in Table 5 spanned the small interval of −0.3 to −0.9 with a mean value of −0.7±0.1 (Asplund et al. 2000). This carbon problem's magnitude is almost independent of the assumed C/He ratio for which the model is constructed, i.e., the difference between the assumed and derived C abundance is maintained as C/He is adjusted. The C I lines included in present syntheses confirm the C problem. With gf-values from the NIST database, these lines demand a gf-value decrease of 0.5–0.8 dex for the eleven stars in Table 5 and the five stars in Table 6.

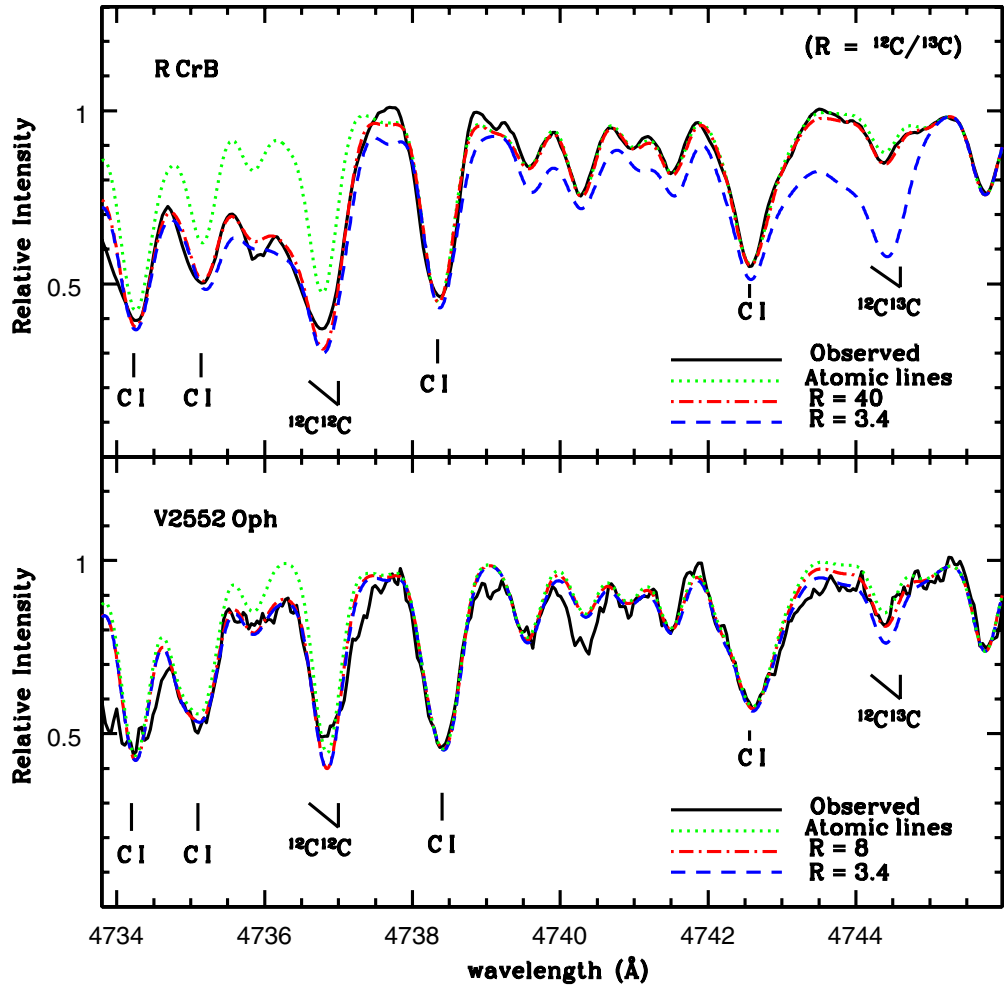

Figure 5. Observed and synthetic spectra of the (1, 0) C_2 bands for R CrB and V2552 Oph. Synthetic spectra are plotted for the values of the isotopic ratios (R) shown in the keys and for a spectrum with only the atomic lines. The positions of the key lines are also marked.

(A color version of this figure is available in the online journal.)

4.1. The $^{12}C/^{13}C$ Ratio

The $^{12}C^{13}C$ molecule's contribution to the spectra is assessed from the (1, 0) band. Unfortunately, there is an unidentified atomic line coincident with the $^{12}C^{13}C$ bandhead. Syntheses show that this atomic line is a major contributor to the stellar feature in most stars. There is also strong atomic blending of the $^{12}C_2$ bandhead but the ^{12}C abundance is provided securely from the (0, 0) and (0, 1) bands. Given these complications, our focus is on determining whether the $^{12}C/^{13}C$ ratio is close to the CN-cycle equilibrium ratio (= 3.4), as might be anticipated for a star produced by the FF scenario, or is a much higher value, as might be provided from the DD scenario. The intensity of a line from the heteronuclear $^{12}C^{13}C$ molecule and the corresponding line from the homonuclear $^{12}C_2$ molecule are related as $I(12-13) = 2I(12-12)/R$ where R is the $^{12}C/^{13}C$ ratio.

Of particular concern to a determination of the $^{12}C/^{13}C$ ratio is the atomic line at 4744.39 Å, which is coincident with the (1, 0) $^{12}C^{13}C$ bandhead. This line is present in the spectrum of γ Cyg, also of the Sun and Arcturus. A line at this wavelength is present in spectra of the hotter RCB stars (V3795 Sgr and XX Cam) whose spectra show no sign of the stronger (0, 0) C_2 band at 5165 Å. The interfering line is unidentified in Hinkle et al.'s (2000) Arcturus atlas. The line list given at the ccp7 Web site[7] identifies the line as arising from a lower level in Fe I at 4.50 eV, but such a line and lower level is not listed by Nave et al. (1994) in their comprehensive study of the Fe I spectrum. The line list given in ccp7 is from Bell & Gustafsson (1989), an unpublished line list. Although this line is assigned in Table 3 to this (fictitious?) Fe I transition, the lack of a positive identification is not a serious issue except, as we note below, perhaps for the minority RCB stars. Given that the gf-value of the line is fixed from the line's strength in spectra of stars that span the temperature range of the RCBs (γ Cyg, Arcturus, and the Sun), alternative identifications have little effect on the predicted strength of the line in an RCB or an HdC star. We assume it is an Fe I line and predict its strength from the inferred gf-value (Table 3) and the Fe abundance derived from a sample of Fe I line in the same region (see above). Table 4 lists our derived Fe abundance, the Fe abundance from Asplund et al. (2000), and the Fe abundance obtained on the assumption that the entire $^{12}C^{13}C$ bandhead is attributable to the Fe I line. There is good agreement between our Fe abundance and that derived from different spectra by Asplund et al. (2000). Perfect agreement would not be expected for several reasons: for example, the stars are somewhat variable even out of decline and our spectra are not those analyzed by Asplund et al. (2000). The

[7] http://ccp7.dur.ac.uk/ccp7/DATA/lines.bell.tar.Z

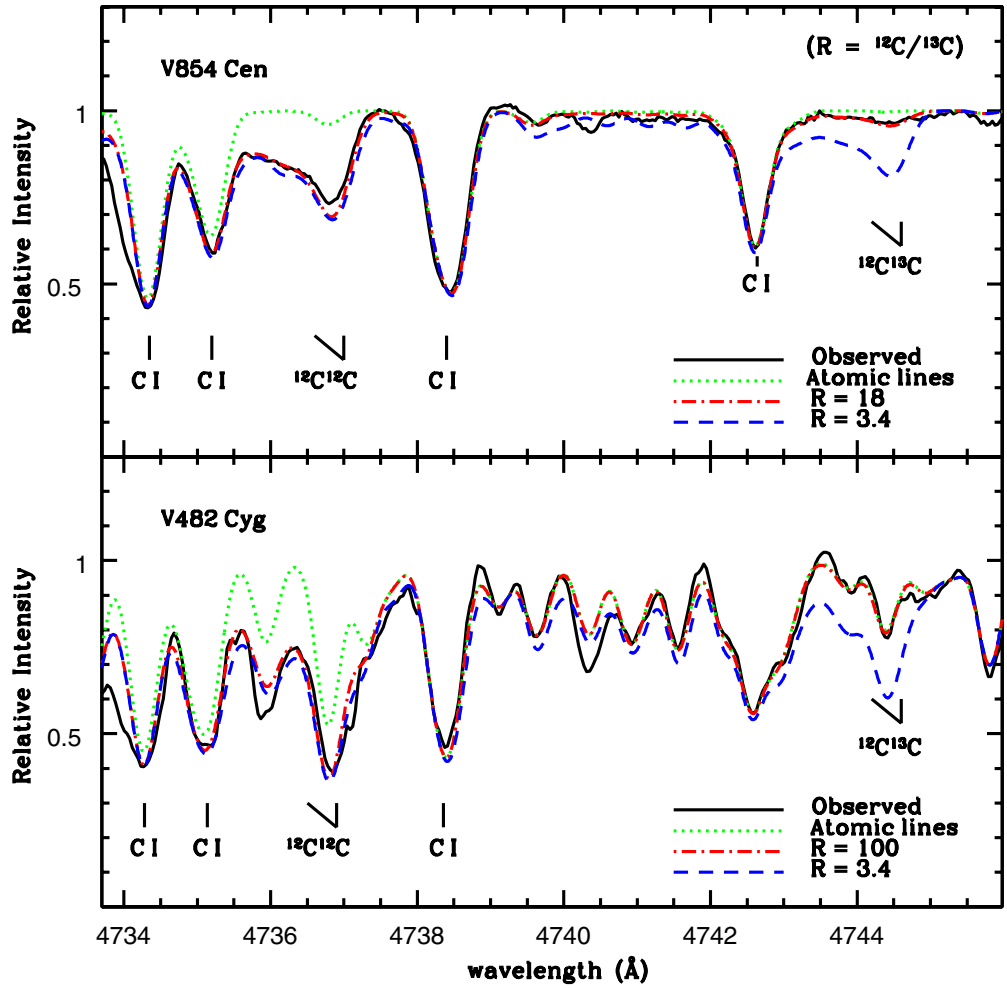

Figure 6. Observed and synthetic spectra of the (1, 0) C_2 bands for V854 Cen and V482 Cyg. Synthetic spectra are plotted for the values of the isotopic ratios (R) shown in the keys and for a spectrum with just the atomic lines. The positions of the key lines are also marked.

(A color version of this figure is available in the online journal.)

difference between the mean Fe abundance and the abundance required to fit the feature at the $^{12}C^{13}C$ bandhead is a rough measure of the inferred molecular contribution to the feature.

Stars are discussed in order of decreasing effective temperature. For all the stars, synthetic spectra are computed for a model with the parameters given in Table 7 and with C/He = 1.0%. The $^{12}C_2$ bands are fitted and then several syntheses are computed for various values of the isotopic ratio R. The estimates of $^{12}C/^{13}C$ ratio are given in Table 7.

VZ Sgr. Observed and synthetic spectra around the (1, 0) band are shown in Figure 3 for this minority RCB star. At 4745 Å, the atomic line (here assumed to be the Fe I line from Table 3) is too weak to account for the observed feature; Table 4 shows that the Fe abundance must be increased by about 1 dex to remove the necessity for a contribution from $^{12}C^{13}C$. A contribution from $^{12}C^{13}C$ seems necessary with $R \simeq 3$–6, a value suggestive of CN-cycling. The observed $^{12}C^{13}C$ band is very weak, and taking into account the S/N, the expected band asymmetry is not evident. The blending Fe I line at the $^{12}C^{13}C$ bandhead further removes the expected asymmetry. However, the blending Fe I line is very weak, the residual spectrum, observed/synthesis (pure C_2 with $R = 4$), suggests the presence of the contaminating line at 4744.39 Å within the uncertainties.

Since the relative metal abundances for VZ Sgr, a minority RCB, are non-solar (Lambert & Rao 1994), the identity of the 4745 Å atomic line may affect the conclusion that this line is an unimportant contributor to the molecular bandhead. For example, VZ Sgr is a minority RCB especially rich in Si and S ([Si/Fe] ∼ [S/Fe] ∼ 2) and a blending line from these elements may reduce the need for a $^{12}C^{13}C$ contribution. However, a search of multiplet tables of Si I (Martin & Zalubas 1983) and S I (Martin et al. 1990; Kaufman & Martin 1993) did not uncover an unwanted blend. Thus, we suppose that VZ Sgr is rich in ^{13}C.

UX Ant. There is a strong (1, 0) $^{12}C_2$ contribution to the spectrum. The predicted profile of the bandhead is broader than the observed head which is distorted by very strong cosmic ray hits on the raw frame. The Fe I line is predicted to be a weak contributor to the feature at the $^{12}C^{13}C$ wavelength. Values of R in the range 14–20 fit the observed feature quite clearly; a synthesis with $R = 3.4$ provides a bandhead that is incompatible with the observed head (Figure 4).

RS Tel. Observed and synthetic spectra shown in Figure 4 indicate that the Fe I line at the $^{12}C^{13}C$ bandhead accounts well for the observed feature and thus $R > 60$ is all that can be said for the carbon isotopic ratio from this spectrum of relatively low S/N.

R CrB. Figure 5 shows observed and synthetic spectra. The Fe I line at the $^{12}C^{13}C$ bandhead accounts for the observed feature. Given that the identity of the line's carrier is uncertain, a conservative view must be that $^{12}C^{13}C$ contributes negligibly

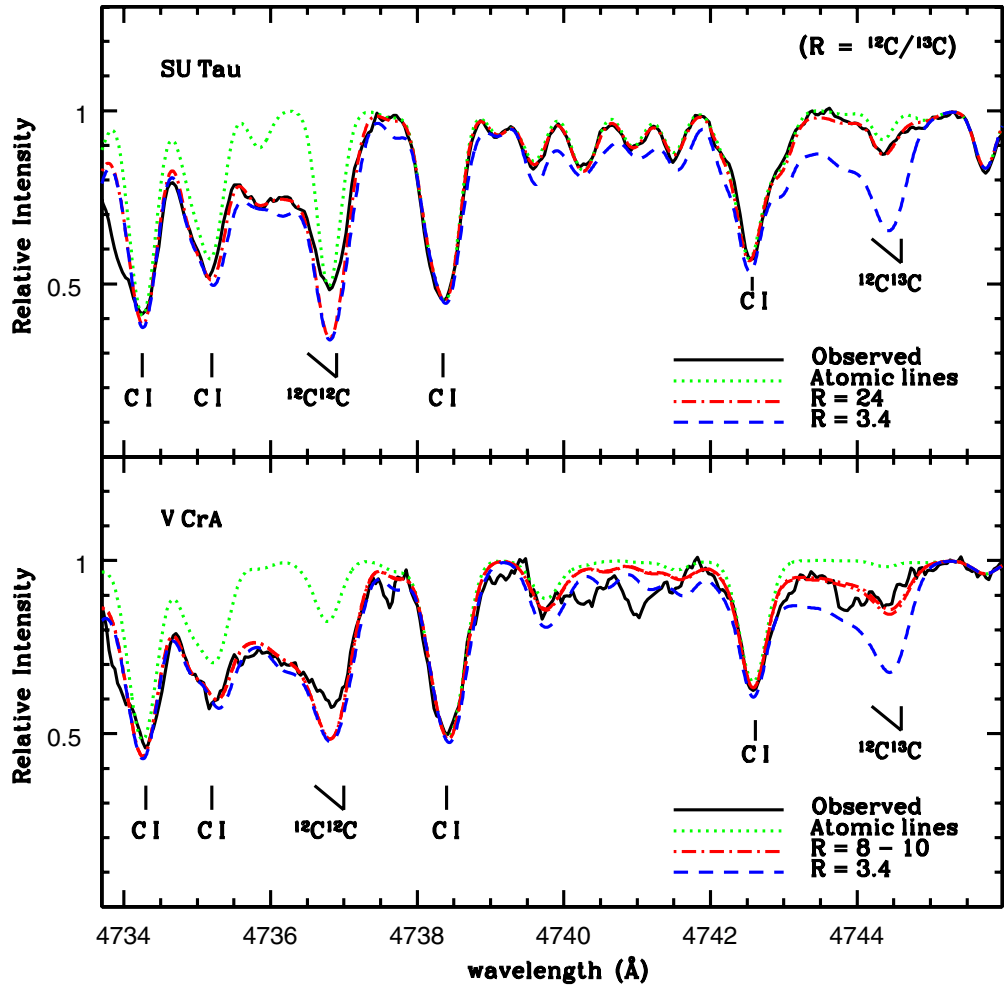

Figure 7. Observed and synthetic spectra of the (1, 0) C_2 bands for SU Tau and V CrA. Synthetic spectra are plotted for the values of the isotopic ratios (R) shown in the keys and for a spectrum with just the atomic lines. The positions of the key lines are also marked.

(A color version of this figure is available in the online journal.)

to the observed feature and $R > 40$ is estimated. It is clear, however, that $R = 3.4$ is excluded as a possible fit.

V2552 Oph. The spectrum of this recently discovered RCB is very similar to that of R CrB (Rao & Lambert 2003) but for its stronger N I lines and weaker C_2 bands (Figure 1 of Rao & Lambert 2003). The $^{12}C_2$ bandhead is very largely obscured by the overlying Fe I line. The apparent $^{12}C^{13}C$ bandhead is almost entirely reproduced by the atomic line. A high R value cannot be rejected, but $R = 3.4$ may be excluded (Figure 5). $R > 8$ is our estimate.

V854 Cen. This RCB with low metal abundances provides a clean spectrum in the region of the (1, 0) Swan bands (Figure 6). The $^{12}C_2$ head is well fitted with a synthetic spectrum. Very high S/N spectra are necessary to set strict limits on the $^{12}C^{13}C$ bandhead, but it is clear that the blending Fe I line is a weak contributor; the Fe abundance must be increased by 1.5 dex to eliminate the need for a $^{12}C^{13}C$ contribution. A ratio $R = 3.4$ is firmly excluded. Values of R in the range 16 to 24 are suggested.

V482 Cyg. The Fe I line accounts well for the observed feature (Figure 6) with a lower limit for the isotopic ratio $R > 100$.

SU Tau. At the $^{12}C^{13}C$ bandhead, the atomic line makes a dominant contribution but the profile of the observed feature suggests that the Swan band is contributing to the blue of the atomic line (Figure 7): R seems to be >24. The $R = 3.4$ synthetic spectrum is clearly rejected as a fit to the observed spectrum.

V CrA. The Fe I line at the $^{12}C^{13}C$ bandhead, and the expected band asymmetry, is seemingly quite unimportant but V CrA is another minority RCB so that the identity of the line's carrier may be relevant here (see above notes on VZ Sgr). The $^{12}C_2$ band is quite strong (Figure 7). With the blending line assigned to Fe I, the observed $^{12}C^{13}C$ bandhead is well fit with $R \simeq 8$–10. Our derived $^{12}C/^{13}C$ ratio is in agreement with the upper limit of the range set by Rao & Lambert (2008) from the same spectrum. Note that an additional line about 0.6 Å to the blue of the $^{12}C^{13}C$ bandhead is seen in this spectrum.

GU Sgr. Presence of the $^{12}C^{13}C$ band is doubtful because atomic lines may account fully for the bandhead and the region just to the blue: R seems to be in the range >40 (Figure 8).

FH Sct. Spectrum synthesis shows that $^{12}C_2$ makes a minor contribution to the observed spectrum (Figure 8) but the ^{12}C abundance may be established from the (0, 0) and (0, 1) bands. The ratio $R > 14$ may be set and the CN-cycle's limit of $R = 3.4$ is excluded.

U Aqr. The (1, 0) $^{12}C_2$ band is so strong (Figure 9) that the uncertainty over R is dominated by the derivation of the ^{12}C abundance from the very saturated (1, 0) $^{12}C_2$ lines. The carbon abundance from (the also saturated) (0, 1) C_2 band is used with

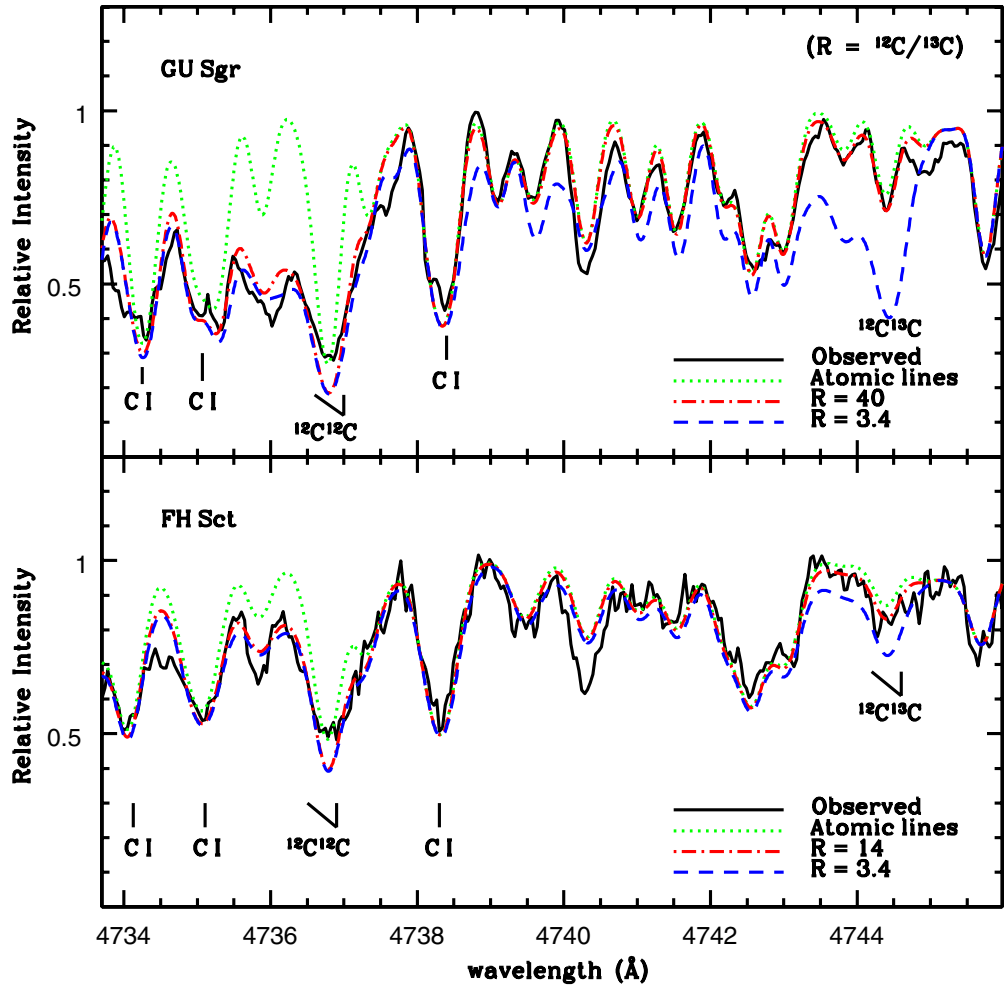

Figure 8. Observed and synthetic spectra of the (1, 0) C_2 bands for GU Sgr and FH Sct. Synthetic spectra are plotted for the values of the isotopic ratios (R) shown in the keys and for a spectrum with just the atomic lines. The positions of the key lines are also marked.

(A color version of this figure is available in the online journal.)

the (1, 0) $^{12}C^{13}C$ blend to derive the $^{12}C/^{13}C$ ratio. The Fe abundance is derived from several lines longward of the (1, 0) $^{12}C^{13}C$ bandhead. A $^{12}C/^{13}C$ ratio in the range 110–120 is obtained.

HdC stars. Syntheses of the (1, 0) band are shown in Figures 10 and 11 for the four HdC stars with the ^{12}C abundance set in each case by the fit to the (0, 1) band (see Figure 12 for a typical fit). In contrast to U Aqr, the $^{12}C^{13}C$ bandhead is well fit by the blending atomic lines with the Fe abundance obtained from lines longward of the bandhead. The derived $^{12}C/^{13}C$ ratio is >100 for HD 137613, >400 for HD 182040, >100 for HD 175893, and >60 for HD 173409.

5. DISCUSSION—C_2 AND THE CARBON PROBLEM

The carbon problem as it appears from the analysis of C I lines is discussed fully by Asplund et al. (2000). In brief, when analyzed with state-of-the-art H-poor model atmospheres (Asplund et al. 1997a) constructed for a C/He ratio (=1%) representative of EHe stars where direct determinations of C and He abundances are possible, the C I lines return a C abundance that is about 0.6 dex less than the input abundance of log ϵ(C) = 9.5. The derived abundance varies little from star to star: 13 of the 17 analyzed RCBs have abundances between 8.8 and 9.0 and the mean from the set of 17 is 8.9±0.2. A similar result is apparent from Tables 5 and 6 where the C abundance from C I lines from our spectrum syntheses is quoted. The discrepancy of 0.6 dex between assumed and derived C abundance is the (C I) carbon problem. As the C/He ratio of a model atmosphere is adjusted, the carbon problem (i.e., the 0.6 dex difference between assumed and derived C abundances) persists until a low C/He reached. This persistence arises because the continuous opacity arises from photoionization of neutral carbon from excited levels.

Tables 5 and 6 also show that the C_2 bands exhibit a carbon problem but one that differs from that shown by the C I lines in several ways: (1) the C abundance from C_2 bands is almost independent of the assumed C/He ratio unlike the abundance from C I lines, (2) the star-to-star spread in C abundances from C_2 bands is larger than found from the C I lines, and (3) the C abundance from C_2 bands is somewhat more sensitive than that from C I lines to changes in the adopted atmospheric parameters as reflected by Table 8 where models spanning the effective temperature and surface gravity uncertainties suggested by Asplund et al. (2000) are considered.

Taken in complete isolation, inspection of Table 5 suggests that a C/He ratio of less than 0.3% can be found for which the ratio adopted in the construction of the model atmosphere is equal to that derived from the C_2 bands. For the RCB stars, Table 5 suggests C/He ratios running from about 0.3% for

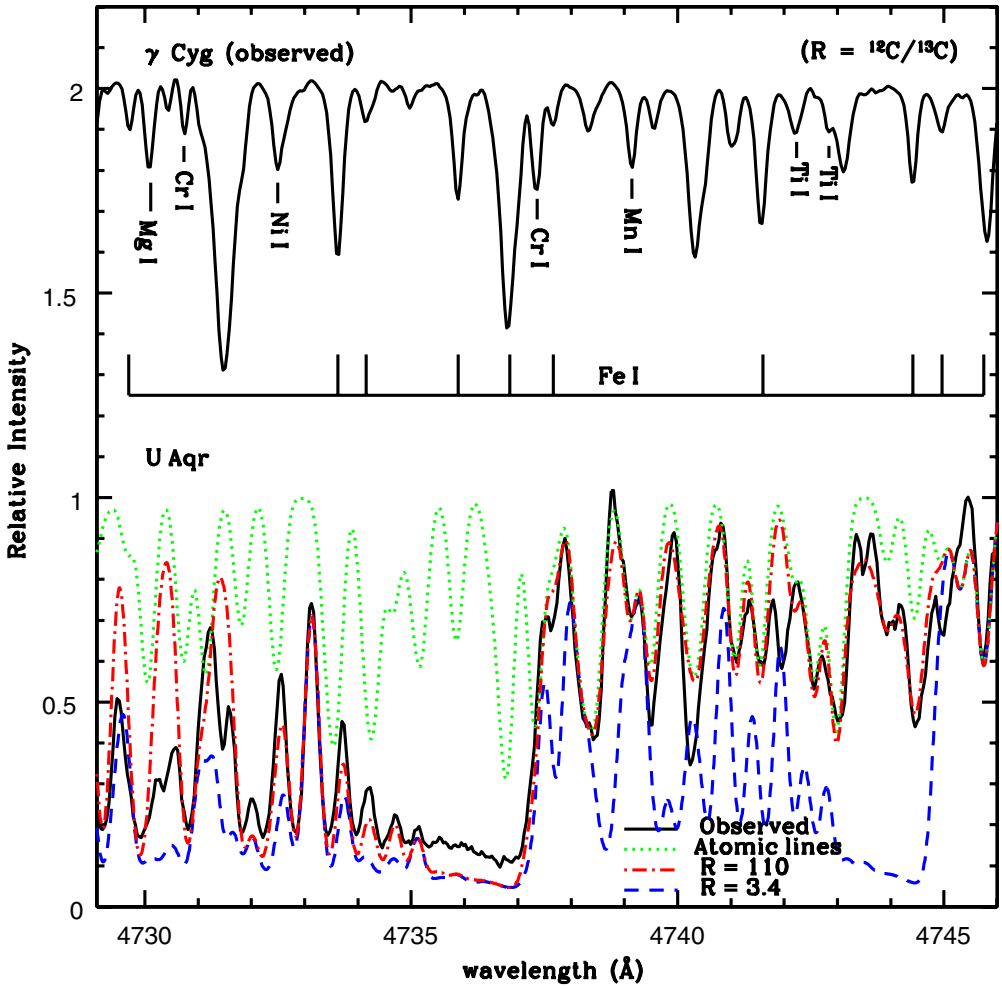

Figure 9. Observed and synthetic spectra of the (1, 0) C_2 bands for U Aqr. Synthetic spectra are plotted for the values of the isotopic ratios (R) shown in the keys and for a spectrum with just the atomic lines. The spectrum of γ Cyg is also plotted—the positions of the key lines are also marked.
(A color version of this figure is available in the online journal.)

VZ Sgr and R CrB down to 0.03% for GU Sgr and FH Sct. For the HdC stars (Table 6), a C/He of slightly larger than 0.1% is suggested. However, Asplund et al. (2000) remark that C/He $\leqslant$ 0.05% is required to eliminate the C I carbon problem by lowering the carbon abundance to the point that photoionization of neutral carbon no longer is the dominant opacity source.

Resolution of the carbon problems by invoking low C/He ratios deserves to be tested fully by constructing model atmospheres with lower C/He ratios and appropriate abundances for other elements and determining the C abundances from C I and C_2 lines. Asplund et al. (2000) recognized this possible way to address the C I carbon problem but discounted it on several grounds: (1) removal of carbon photoionization as the dominant continuous opacity makes it difficult to account for the near-uniformity of the C I equivalent widths across the RCB sample, especially as O abundance varies from star to star; (2) an inverse carbon problem is created for the C II lines at 6578 Å and 6582 Å, which are seen in the hottest RCBs; and (3) these low C/He ratios for RCB stars are at odds with the higher ratios obtained directly from He and C lines for EHe stars, which one assumes are intimate relatives of the RCB and HdC stars. Asplund et al. (2000) noted that published analyses of EHe stars gave the mean C/He = 0.8 $\pm$ 0.3% over a range 0.3%–1.0% with three unusual EHe stars providing much lower ratios (0.002%–0.2%). Pandey et al. (2006) confirmed the C/He ratios for the leading group of EHe stars. From the following references (Pandey et al. 2001, 2006; Pandey & Lambert 2011; Jeffery et al. 1998, 1999; Drilling et al. 1998; Pandey & Reddy 2006; Jeffery & Heber 1993; Harrison & Jeffery 1997), which also include the recent analyses of these EHe stars, the mean value of C/He = 0.6 $\pm$ 0.3% is noted.

The RCB–EHe mismatch of their C/He ratios invites two responses: (1) the carbon problems for the RCB stars should be resolved on the assumption that their C/He ratios and those of the EHe stars span similar ranges, or (2) as a result of different evolutionary paths, the C/He ratios of RCB and EHe stars span different ranges.

After considering a suite of possible explanations for their carbon problem, Asplund et al. (2000) proposed that the actual atmospheres of the RCB stars differed from the theoretical atmospheres in that the temperature gradient was flatter than predicted. Hand-crafted atmospheres were shown to solve the C I carbon problem. However, the issue of accounting for the additional heating and cooling of the hand-crafted atmospheres was left unresolved. In principle, the change in the temperature structure—a heating at modest optical depths—will require a higher C abundance to account for the C_2 bands so that the C I and C_2 carbon problems might both be eliminated.

Further exploration of the carbon problem was pursued by Pandey et al. (2004) who observed the 8727 Å and 9850 Å [C I]

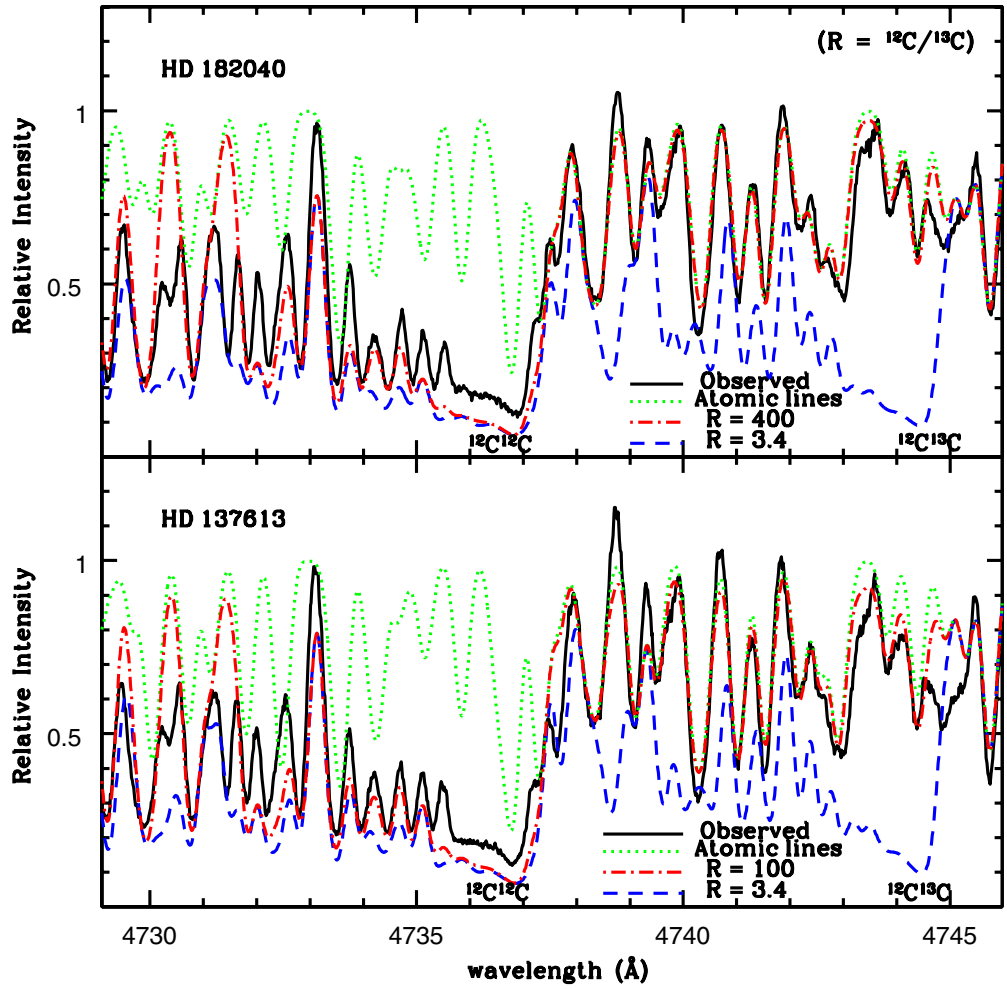

Figure 10. Observed and synthetic spectra of the (1, 0) C_2 bands for HD 182040 and HD 137613. Synthetic spectra are plotted for the values of the isotopic ratios (R) shown in the keys and for a spectrum with just the atomic lines. The positions of the key lines are also marked.
(A color version of this figure is available in the online journal.)

lines in a sample of RCB stars. The 8727 Å line gives a more severe carbon problem than the C I lines, say 1.2 dex versus 0.6 dex for C/He = 1.0% model atmospheres. In part, this difference might be reduced by a revision of the effective temperature scale because the [C I] line being of low excitation potential has a temperature dependence relative to the continuous carbon opacity from highly excited levels. The 9850 Å line may give a similar carbon problem to the C I lines or the forbidden line may be blended with an unidentified line. To account for the 8727 Å carbon problem, Pandey et al. (2004) considered introducing a chromospheric temperature rise to the theoretical model photospheres. Such a chromosphere with LTE produces emission at the C_2 bandheads and offers a qualitative explanation for the fact that the best-fitting synthetic spectra from the theoretical photospheres (i.e., no chromospheric temperature rise) are deeper than the observed spectra at the bandheads.

Analysis of the C_2 bands suggests a novel clue to the C_2 carbon problem. As Figure 13 shows, the C abundance from the C_2 bands is correlated with the O abundance derived by Asplund et al. (2000) from O I and/or [O I] lines. The points are distributed about the relation C/O $\sim$ 1. (The C abundance from the C I lines is not well correlated with the O abundance and most points fall below the C/O = 1 locus). In Figure 14, the EHe stars are plotted along with RCB stars. The RCB stars may connect those EHe stars of very low C/He with the majority of higher C/He.

Perhaps a more powerful clue is the fact that the Fe abundance of the RCB and HdC stars is uniformly sub-solar. The mean Fe abundance excluding the minority RCBs is 6.5 or 1.0 dex less than the solar Fe abundance. EHe stars show a similar spread and mean Fe abundance of 6.7 (Jeffery et al. 2011).

6. DISCUSSION—THE $^{12}C/^{13}C$ RATIO AND THE ORIGIN OF THE RCBs

Discussion of the determinations of the $^{12}C/^{13}C$ ratio can be focused on three main points.

First, the ratio is low in the two minority RCBs VZ Sgr and V CrA. Unless there is an unidentified line from an element with an overabundance in a minority RCB star, VZ Sgr has a $^{12}C/^{13}C$ ratio equal within the measurement uncertainty to the equilibrium ratio for the H-burning CN-cycle. The ratio is higher ($\simeq$8) for V CrA but considerably lower than the upper limits set for majority RCBs. (Rao & Lambert 2008 gave the ratio as 3.4 for V CrA but apparently did not include the factor of two arising from the fact that $^{12}C^{13}C$ is not a homonuclear molecule, i.e., 3.4 should be 6.8.) In some respects, V854 Cen is

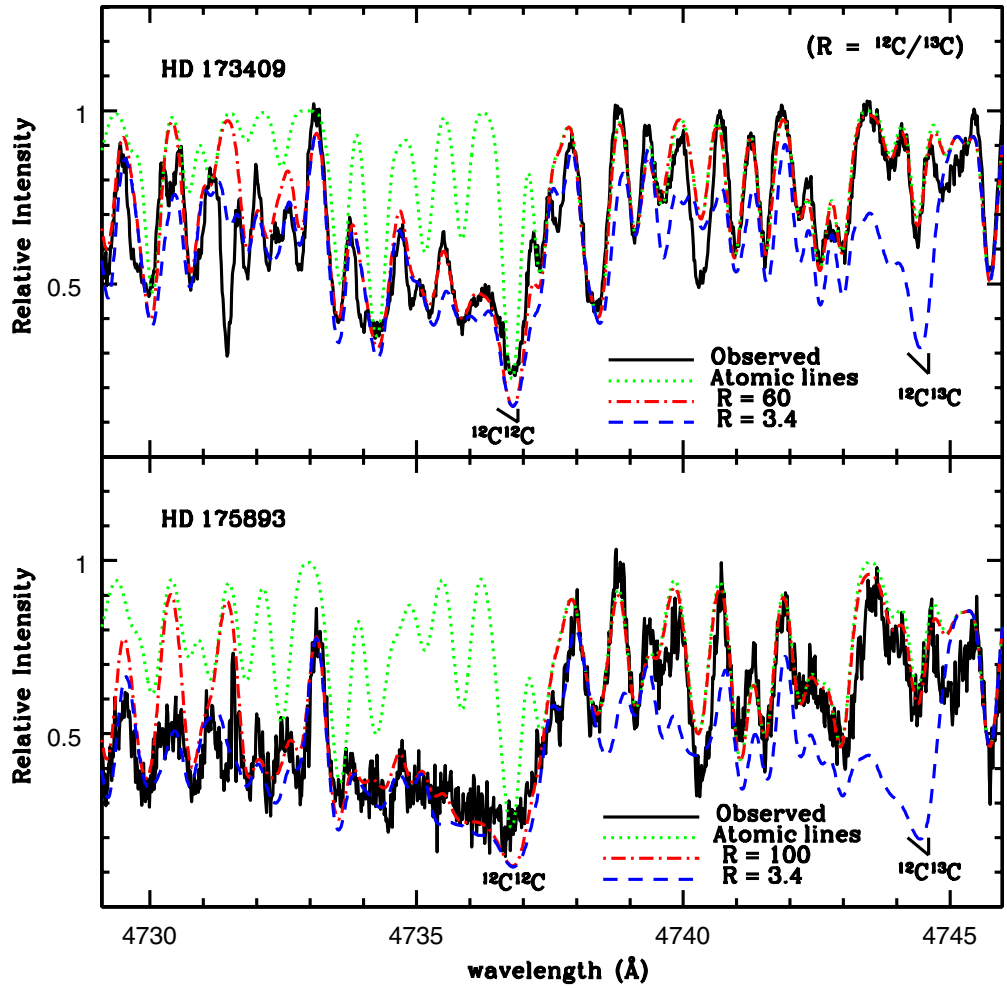

Figure 11. Observed and synthetic spectra of the (1, 0) C_2 bands for HD 173409 and HD 175893. Synthetic spectra are plotted for the values of the isotopic ratios (R) shown in the keys and for a spectrum with just the atomic lines. The positions of the key lines are also marked.

(A color version of this figure is available in the online journal.)

a minority RCB star and its $^{12}C/^{13}C$ ratio of 18 is also generally lower than representative upper limits for majority RCB stars.

Second, the $^{12}C/^{13}C$ ratio for all majority RCBs is much larger than the equilibrium ratio for the CN-cycle.[8]

Third, there appears to be a range in the $^{12}C/^{13}C$ ratios among majority RCBs. The star with the lowest ratio appears to be UX Ant (Figure 4) for which the predicted blend of atomic lines at the (1, 0) $^{12}C^{13}C$ bandhead accounts for less than half of the strength of the observed absorption feature. Similarly for U Aqr, the atomic lines at the bandhead account for about half of the observed feature but because the C_2 lines are strong the isotopic bandhead translates to the ratio $^{12}C/^{13}C \simeq 110$. For these cases at least, it seems likely that the $^{12}C^{13}C$ bandhead is present in our spectra. Within the uncertainties associated with the blend of atomic lines, other RCBs yield a lower limit to the isotopic ratio. This limit is highest for the HdCs where the C_2 bands are very strong. Note how the atomic lines account remarkably well for the observed spectrum between the $^{12}C_2$ and $^{12}C^{13}C$ (1, 0) bandheads.

Our results are in good agreement with published results for the few stars previously analyzed (Table 7). In the case of R CrB, Cottrell & Lambert (1982) determined a lower limit of 40 from the C_2 (0, 1) band. Fujita & Tsuji (1977) from spectra of the CN Red system set lower limits of 500 for HD 137613 and >100 for HD 182040. The latter limit was also reported by Climenhaga (1960) from high-resolution photographic spectra of C_2 bands. Lower limits set by García-Hernández et al. (2009, 2010) are not competitive with those from CN or our limits from C_2.

Prospects for a low $^{12}C/^{13}C$ ratio in the atmosphere of a product of the DD scenario are dim. In the scenario's cold version (i.e., no nucleosynthesis as a result of the merger), the C is provided by the He shell of the C–O white dwarf and quite likely also by layers of the C–O core immediately below the He shell. The latter contribution will be devoid of ^{13}C. In the He shell, ^{13}C may be present in the outermost layers as a result of penetration of protons from the H-rich envelope of the former AGB star into the He shell. Very slow penetration results in the build up of a $^{12}C/^{13}C$ ratio of about 3 and inhibits somewhat the conversion of the ^{13}C to ^{14}N, as usually occurs in the CN-cycle. This mechanism sustains the favored neutron source for the s-process in AGB stars; the $^{13}C(\alpha, n)^{16}O$ is the neutron source. The He is provided almost entirely by the He white dwarf which will have very little carbon but abundant nitrogen as a result of H-burning by the CNO-cycles.

[8] We note that Goswami et al.'s (2010) observation that the ratio is about 3.4 for U Aqr is incompatible with our spectra by simple inspection of Figure 9.

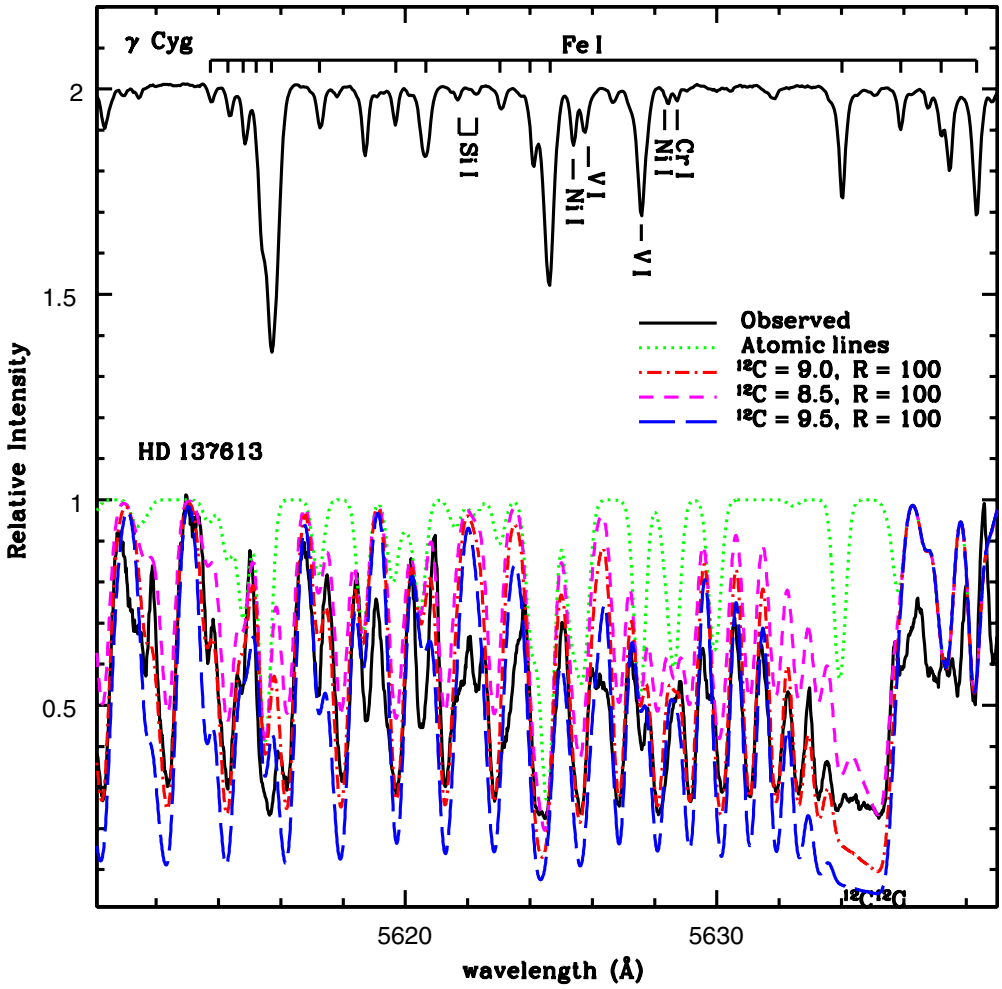

Figure 12. Observed and synthetic spectra of the (0, 1) C_2 band for HD 137613. Synthetic spectra are plotted for different values of the C abundance—see key on the figure. The spectrum of the γ Cyg is plotted with the positions of the key lines marked.
(A color version of this figure is available in the online journal.)

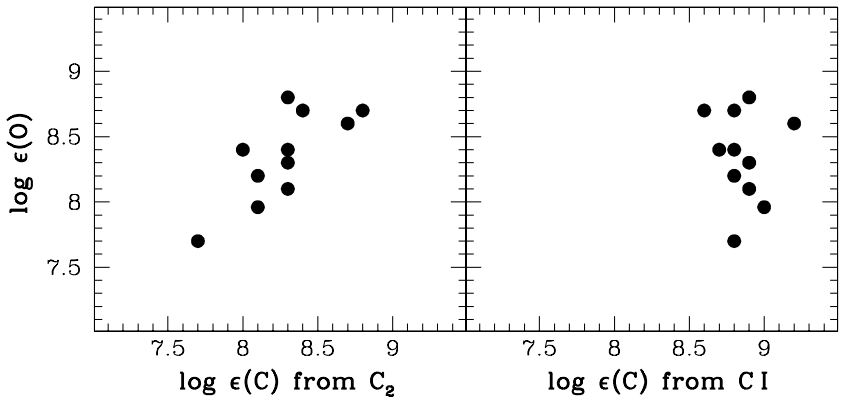

Figure 13. Plot of log ϵ(C), from C_2 bands and C I lines vs. log ϵ(O) for RCB stars. log ϵ(O) and log ϵ(C), from C I lines, are from Asplund et al. (2000).

A cold merger of the He white dwarf with the He shell of the C–O white dwarf results in a C/He ratio (see Pandey & Lambert 2011, Equation (1))

$$\frac{\mathrm{C}}{\mathrm{He}} \simeq \frac{\mathrm{A(He)}}{\mathrm{A(C)}} \frac{\mu(\mathrm{C})_{\mathrm{C-O:He}} M(\mathrm{C-O:He})}{M(\mathrm{He})}, \qquad (1)$$

where $\mu(\mathrm{C})_{\mathrm{C-O:He}}$ is the mass fraction of ^{12}C in the He shell, M(C–O:He) is the mass of the He shell, and M(He) is the mass of the He white dwarf. With plausible values for the quantities on the right-hand side of the equation, i.e., $\mu(\mathrm{C})_{\mathrm{C-O:He}} \simeq 0.2$, M(C–O:He) $\simeq 0.02\ M_\odot$, and M(He) $\simeq 0.3\ M_\odot$, one obtains C/He $\simeq 0.4\%$, a value at the lower end of the C/He range found for EHe stars. Additional ^{12}C is likely provided by mixing with the layers of the C–O white dwarf immediately below the He shell.

The attendant ^{12}C/^{13}C ratio will be a maximum if these latter contributions are absent. Then, this ratio will depend on the fraction of the He shell over which ^{13}C is abundant (relative to

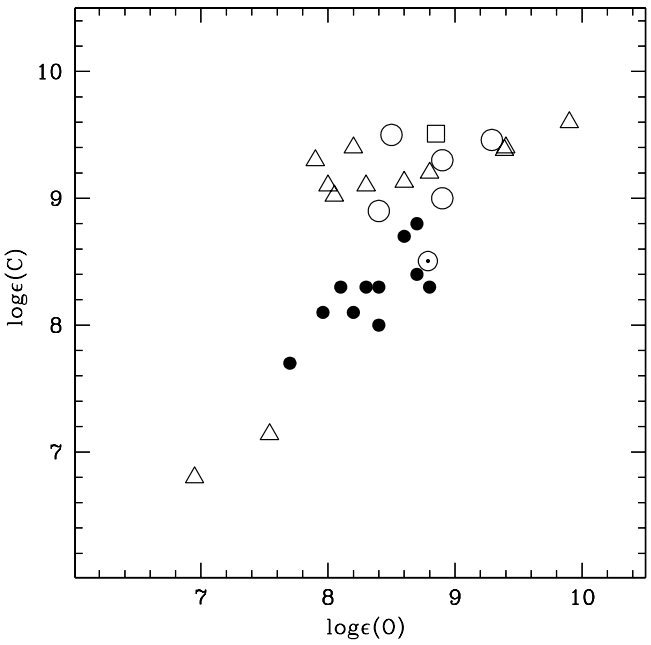

Figure 14. Plot of log ϵ(C) from C_2 bands vs. log ϵ(O) (Asplund et al. 2000) for RCB stars. Also shown are the EHe stars. Our sample of eleven RCBs are represented by filled circles. Five cool EHes are represented by open circles (Pandey et al. 2001, 2006; Pandey & Reddy 2006). Twelve hot EHes are represented by open triangles (Drilling et al. 1998; Harrison & Jeffery 1997; Jeffery et al. 1998, 1999; Pandey & Lambert 2011). DY Cen, the hot minority RCB (Jeffery & Heber 1993), is represented by open squares. "⊙" represents the Sun.

^{12}C), say $^{12}C/^{13}C \sim 3/f_{13}$ where f_{13} is the fraction of the He shell which is rich in ^{13}C. For $f_{13} \sim 0.1$ and 0.01, the predicted isotopic ratio is 30 and 300, respectively. These estimates must be increased when the mixing at the merger includes the layers of the C–O white dwarf immediately below the He shell.

At present, there are no reliable ab initio calculations of the mass of the ^{13}C-rich layer in the He shell of an AGB star. Additionally, one is making a bold assumption that the He shell of the C–O white dwarf which accepts merger with the He white dwarf resembles the He shell of an AGB star. Mass estimates relevant to an AGB star may be obtained by the fit to observed *s*-process abundances. Gallino et al. (1998) suppose that the ^{13}C-rich layer amounts to about 1/20 of the mass in a typical thermal pulse occurring in the He shell. With $f_{13} \simeq 0.05$, the isotopic ratio is 60. Interestingly, this is consistent with our inferred range. This will increase as the C–O white dwarf contributes to the mixing. Destruction of ^{13}C by α particles may occur in a "hot" phase during the merger and thus also raise the isotopic ratio; the $^{13}C(\alpha, n)$ destruction rate is roughly a factor of 100 faster than the $^{14}N(\alpha, \gamma)$ rate providing ^{18}O. The low isotopic ratio for minority RCB stars—VZ Sgr and V CrA—are unexplained as are their distinctive elemental abundances.

7. CONCLUDING REMARKS

The C_2 Swan bands are present in spectra of the HdC stars and in all but the hottest RCB stars. Analysis of these bands provides an alternative to the C I lines of providing estimates of the C abundance and in addition provides an opportunity to estimate the $^{12}C/^{13}C$ ratio. When analyzed with Uppsala model atmospheres, the C_2 bands return a C abundance that is almost independent of the C/He ratio assumed in construction of the model atmosphere. If consistency between assumed and derived C abundances is demanded, the C_2 bands imply C/He ratios across the RCB and HdC sample run in the range 0.03%–0.3%, a range that is notably lower than the range 0.3%–1.0% found from a majority of EHes. This mismatch, if not a reflection of different modes of formation, implies that the C abundances for RCB and HdC stars are subject to a systematic error. Therefore, it appears that a version of the carbon problem affecting the C I lines (Asplund et al. 2000) applies to the C_2 lines. Although alternative explanations cannot yet be totally eliminated, it appears that higher-order methods of model atmosphere construction are needed in order to check that Asplund et al.'s suggestion of the real atmospheres have a flatter temperature gradient than predicted by present state-of-the-art model atmospheres. Nonetheless, that the carbon abundances derived from C_2 Swan bands are the real measure of the carbon abundances in these stars cannot be ruled out.

There is evidence for the presence of detectable amounts of ^{13}C in the spectra of a few RCB stars and especially for the minority RCB stars. For the other RCBs and the HdC stars, lower limits are set on the carbon isotopic ratio. Apart from the minority RCB stars, the estimates of the carbon isotopic ratio are consistent with simple predictions for a cold merger of a He white dwarf with a C–O white dwarf.

The minority RCB stars are an enigma. Their distinctive pattern of elemental abundances remains unaccounted for: for example, V CrA has an Fe deficiency of 2 dex but [Si/Fe] ∼ [S/Fe] ∼ [Sc/Fe] ≃ 2 with [Na/Fe] ∼ [Mg/Fe] ∼ 1 (Rao & Lambert 2008). Added to these anomalies, the $^{12}C/^{13}C$ ratio is much lower than found for the majority RCB stars unless the (1, 0) Swan $^{12}C^{13}C$ bandhead is blended with an as-yet-unidentified atomic line whose strength is unsuspected from examination of the spectra of majority RCB stars. This enigma calls for additional observational insights.

We thank the referee for a fine report. We thank Kjell Eriksson and Anibal García-Hernández for the H-deficient models of the cool stars, particularly Kjell Eriksson for providing these models in our required format. We thank Kameswara Rao for providing us with the spectra of V854 Cen and V CrA. We also thank Nils Ryde for making available a C_2 line list sample. D.L.L. wishes to thank the Robert A. Welch Foundation of Houston, TX for support through grant F-634.

REFERENCES

Asplund, M., Grevesse, N., Sauval, A. J., Allende Prieto, C., & Blomme, R. 2005, A&A, 431, 693
Asplund, M., Grevesse, N., Sauval, A. J., & Scott, P. 2009, ARA&A, 47, 481
Asplund, M., Gustafsson, B., Kiselman, D., & Eriksson, K. 1997a, A&A, 318, 521
Asplund, M., Gustafsson, B., Lambert, D. L., & Kameswara Rao, N. 1997b, A&A, 321, L17
Asplund, M., Gustafsson, B., Lambert, D. L., & Rao, N. K. 2000, A&A, 353, 287
Bell, R. A., & Gustafsson, B. 1989, MNRAS, 236, 653
Clayton, G. C., & De Marco, O. 1997, AJ, 114, 2679
Clayton, G. C., Geballe, T. R., Herwig, F., Fryer, C., & Asplund, M. 2007, ApJ, 662, 1220
Clayton, G. C., Herwig, F., Geballe, T. R., et al. 2005, ApJ, 623, L141
Climenhaga, J. L. 1960, AJ, 65, 50
Cottrell, P. L., & Lambert, D. L. 1982, ApJ, 261, 595
Drilling, J. S., Jeffery, C. S., & Heber, U. 1998, A&A, 329, 1019
Fujita, Y., & Tsuji, T. 1977, PASJ, 29, 711
Gallino, R., Arlandini, C., Busso, M., et al. 1998, ApJ, 497, 388
García-Hernández, D. A., Hinkle, K. H., Lambert, D. L., & Eriksson, K. 2009, ApJ, 696, 1733
García-Hernández, D. A., Lambert, D. L., Kameswara Rao, N., Hinkle, K. H., & Eriksson, K. 2010, ApJ, 714, 144

Gonzalez, G., Lambert, D. L., Wallerstein, G., et al. 1998, ApJS, 114, 133
Goswami, A., Karinkuzhi, D., & Shantikumar, N. S. 2010, ApJ, 723, L238
Gustafsson, B., Edvardsson, B., Eriksson, K., et al. 2008, A&A, 486, 951
Harrison, P. M., & Jeffery, C. S. 1997, A&A, 323, 177
Herzberg, G., & Phillips, J. G. 1948, ApJ, 108, 163
Hinkle, K., Wallace, L., Valenti, J., & Harmer, D. (ed.) 2000, Visible and Near Infrared Atlas of the Arcturus Spectrum 3727-9300 A (San Francisco, CA: ASP)
Iben, I., Jr., & Tutukov, A. V. 1985, ApJS, 58, 661
Jeffery, C. S., Hamill, P. J., Harrison, P. M., & Jeffers, S. V. 1998, A&A, 340, 476
Jeffery, C. S., & Heber, U. 1993, A&A, 270, 167
Jeffery, C. S., Hill, P. W., & Heber, U. 1999, A&A, 346, 491
Jeffery, C. S., Karakas, A. I., & Saio, H. 2011, MNRAS, 414, 3599
Kaufman, U., & Martin, W. C. 1993, J. Phys. Conf. Ser., 22, 279
Lambert, D. L., & Rao, N. K. 1994, J. Astrophys. Astron., 15, 47
Luck, R. E., & Lambert, D. L. 1981, ApJ, 245, 1018
Lundmark, K. 1921, PASP, 33, 314
Martin, W. C., & Zalubas, R. 1983, J. Phys. Chem. Ref. Data, 12, 323
Martin, W. C., Zalubas, R., & Musgrove, A. 1990, J. Phys. Chem. Ref. Data, 19, 821
Moore, Ch. E. 1993, Tables of Spectra of Hydrogen, Carbon, Nitrogen, and Oxygen Atoms and Ions, CRC Series in Evaluated Data in Atomic Physics, ed. J. W. Gallagher (Boca Raton, FL: CRC Press)
Naulin, C., Costes, M., & Dorthe, G. 1988, Chem. Phys. Lett., 143, 496
Nave, G., Johansson, S., Learner, R. C. M., Thorne, A. P., & Brault, J. W. 1994, ApJS, 94, 221
Pandey, G. 2006, ApJ, 648, L143
Pandey, G., Kameswara Rao, N., Lambert, D. L., Jeffery, C. S., & Asplund, M. 2001, MNRAS, 324, 937
Pandey, G., & Lambert, D. L. 2011, ApJ, 727, 122
Pandey, G., Lambert, D. L., Jeffery, C. S., & Rao, N. K. 2006, ApJ, 638, 454
Pandey, G., Lambert, D. L., & Rao, N. K. 2008, ApJ, 674, 1068
Pandey, G., Lambert, D. L., Rao, N. K., et al. 2004, MNRAS, 353, 143
Pandey, G., & Reddy, B. E. 2006, MNRAS, 369, 1677
Pavlenko, Y. V., Geballe, T. R., Evans, A., et al. 2004, A&A, 417, L39
Pesic, D. S., Vujisic, B. R., Rakotoarijimy, D., & Weniger, S. 1983, J. Mol. Spectrosc., 100, 245
Peterson, R. C., Dalle Ore, C. M., & Kurucz, R. L. 1993, ApJ, 404, 333
Phillips, J. G., & Davis, S. P. (ed.) 1968, The Swan System of the C2 Molecule. The Spectrum of the HgH Molecule (Berkeley, CA: Univ. California Press)
Rao, N. K., & Lambert, D. L. 2003, PASP, 115, 1304
Rao, N. K., & Lambert, D. L. 2008, MNRAS, 384, 477
Rao, N. K., Sriram, S., Jayakumar, K., & Gabriel, F. 2005, J. Astrophys. Astron., 26, 331
Renzini, A. 1979, in Stars and Star Systems, ed. B. E. Westerlund (Astrophysics and Space Science Library, Vol. 75; Dordrecht: Reidel), 155
Renzini, A. 1990, in ASP Conf. Ser. 11, Confrontation Between Stellar Pulsation and Evolution, ed. C. Cacciari & G. Clementini (San Francisco, CA: ASP), 549
Russo, R. E., Bol'Shakov, A. A., Mao, X., et al. 2011, Spectrochim. Acta, 66, 99
Schmidt, T. W., & Bacskay, G. B. 2007, J. Chem. Phys., 127, 234310
Stawikowski, A., & Greenstein, J. L. 1964, ApJ, 140, 1280
Tull, R. G., MacQueen, P. J., Sneden, C., & Lambert, D. L. 1995, PASP, 107, 251
Urdahl, R. S., Bao, Y., & Jackson, W. M. 1991, Chem. Phys. Lett., 178, 425
Warner, B. 1967, MNRAS, 137, 119
Webbink, R. F. 1984, ApJ, 277, 355